NIST Technical Note 1813

Effect of Concentration on R134a/Al2O3 Nanolubricant Mixture Boiling on a Reentrant Cavity Surface with Extensive Measurement and Analysis Details

Mark A. Kedzierski

http://dx.doi.org/10.6028/NIST.TN.1813

National Institute of Standards and Technology
U.S. Department of Commerce

NIST Technical Note 1813

Effect of Concentration on R134a/Al_2O_3 Nanolubricant Mixture Boiling on a Reentrant Cavity Surface with Extensive Measurement and Analysis Details

Mark A. Kedzierski
Energy and Environment Division
Engineering Laboratory

http://dx.doi.org/10.6028/NIST.TN.1813

September 2013

U.S. Department of Commerce
Penny Pritzker, Secretary

National Institute of Standards and Technology
Patrick D. Gallagher, Under Secretary of Commerce for Standards and Technology and Director

National Institute of Standards and Technology Technical Note 1813
Natl. Inst. Stand. Technol. Tech. Note 1813, 51 pages (September 2013)
CODEN: NTNOEF
http://dx.doi.org/10.6028/NIST.TN.1813

Effect of Concentration on R134a/Al_2O_3 Nanolubricant Mixture Boiling on a Reentrant Cavity Surface with Extensive Measurement and Analysis Details

M. A. Kedzierski
National Institute of Standards and Technology
Bldg. 226, Rm B114
Gaithersburg, MD 20899
Phone: (301) 975-5282
Mark.Kedzierski@NIST.gov

ABSTRACT

This paper quantifies the influence of Al_2O_3 nanoparticles on the pool boiling performance of R134a/polyolester mixtures on a Turbo-BII-HP boiling surface. Nanolubricants with 10 nm diameter Al_2O_3 nanoparticles of various volume fractions (1.6 %, 2.3 %, and 5.1 %) in the base polyolester lubricant were mixed with R134a at two different mass fractions (0.5 % and 1 %). The study showed that nanolubricants can improve R134a boiling on a reentrant cavity surface as long as the nanoparticles remain well dispersed in the lubricant and are at sufficiently large concentration. For example, three of the refrigerant/nanolubricant mixtures with the smallest nanoparticle mass fraction exhibited average enhancements over the entire heat flux range of approximately 10 %. However, when the nanoparticle mass fraction was increased to a point that likely encouraged agglomeration, an average heat transfer degradation of approximately 14 % resulted. An expression for the nanoparticle surface density was developed for the Turbo-BII-HP surface for use in an existing model for predicting refrigerant/nanolubricant boiling. For heat fluxes greater than 35 kWm^{-2}, the model was within 0.5 %, 21 %, and 16 % of the measured heat flux ratios for mixtures with increasing nanoparticle surface density, respectively. The correspondence between the increases in the model deviation with the increase in nanoparticle surface density may be due to the increased propensity for agglomeration at greater nanoparticle surface density.

Keywords: additives, aluminum oxide, boiling, enhanced heat transfer, nanolubricant, nanotechnology, refrigerants, refrigerant/lubricant mixtures, structured surface

TABLE OF CONTENTS

LIST OF FIGURES

LIST OF TABLES

INTRODUCTION

Recent advances in nanofluids research have demonstrated the potential for using nanofluids in heat transfer equipment to enhance its efficiency and/or performance. An advantage of nanofluids is that nanoparticle materials can be very inexpensive and the technology for producing nanofluids is mature, especially for viscous liquids. In general, viscous liquids produce stable nanofluids due to low settling velocities. Despite this, both Wu et al. (2008) and Park and Jung (2007) have observed significant boiling enhancements by adding nanoparticles to a fluid with a relatively low viscosity, i.e., a refrigerant. As one would expect, without constant mixing, the probability of nanoparticle settling is greater for a low viscosity fluid than for a fluid with a large viscosity. Accordingly, Wu et al. (2008), Trisaksri and Wongwises (2009), and Das et al. (2003) attributed the boiling degradations with nanoparticles that they observed, for low viscosity fluids like refrigerants and water, to nanoparticle deposition on the boiling surface. For this reason, lubricants with dispersed nanoparticles, i.e., nanolubricants, can offer the possibility of improving the suspension of the nanoparticles due to the favorable viscosity of lubricants. In addition, the lubrication of friction surfaces can be improved (Lee et al., 2009) like those that exist in air-conditioning compressor with the use of nanolubricants.

Studies by Henderson et al. (2010), Bi et al. (2007a), Peng et al. (2011), Hu (2013), and Kedzierski (2008) have explored the use of nanolubricants as a means for improving efficiencies of air-conditioning and refrigeration equipment. For low flow qualities, Henderson et al. (2010) have shown that CuO nanoparticles can improve the flow boiling heat transfer of refrigerant/lubricant mixtures by as much as 76 % and that the lubricant can act as a necessary dispersant. Peng et al. (2010) have shown that diamond nanolubricants can improve refrigerant/lubricant pool boiling by as much as 63 %. Similarly, Copper-oxide nanoparticles have also been shown to improve refrigerant/lubricant pool boiling by as much as 245 % (Kedzierski and Gong, 2009). The key to the boiling enhancement for refrigerants as caused by nanolubricants is that the nanoparticles inhabit the viscous lubricant excess layer that covers evaporator surface and stably interact with nucleating bubbles to cause enhanced bubble growth (Kedzierski, 2009). In addition, the combined effects of nanoparticles on heat transfer and compressor performance were illustrated by Bi et al. (2007b) when they showed that nanolubricants produced energy savings of more than 25 % in domestic refrigerators. Aluminum-oxide nanoparticles have produced similar enhancements for refrigerant/lubricant boiling (Kedzierski, 2011, 2012a). These preceding studies suggest that it is worthwhile to investigate the potential benefits of nanolubricants for large commercial chillers.

Kedzierski (2001a) has shown that the lubricant viscosity and density influence the performance of boiling refrigerant/nanolubricant mixtures and are required parameters for its prediction (Kedzierski, 2012a). Because of works like Eastman et al. (2001), nanofluids immediately bring to mind the benefits of increased thermal conductivity as induced by the nanoparticles. However, when considering refrigerant/nanolubricant boiling, the improvement associated with increased thermal conductivity is generally less than 20 % of the total boiling enhancement (Kedzierski, 2008). Most of the enhancement is caused by an exchange of momentum between the nanoparticles and the bubbles (Kedzierski, 2011, 2012a).

The pool boiling heat transfer model that was developed in Kedzierski (2012a) showed that the heat transfer depends on, among other things, the nanoparticle surface density in the lubricant excess layer that exists on the boiling surface (Kedzierski, 2012a). In fact, if the nanoparticle concentration is less than a critical value, boiling heat transfer can be degraded because there are insufficient numbers of nanoparticles remaining in the lubricant excess layer to interact with bubbles (Kedzierski, 2009). Likewise, the boiling enhancement with nanolubricants is surface dependent given that a similar study showed that the same nanolubricant caused on average a 12 % boiling heat transfer degradation on a surface with reentrant cavities (Kedzierski, 2012b).

Consequently, the purpose of the present investigation was to determine if the performance of reentrant cavity type surfaces, like the Turbo-BII-HP, could be enhanced with sufficiently concentrated nanolubricants and, if so, would the enhancement follow the refrigerant/nanolubricant boiling theory developed in Kedzierski (2012a). To achieve this, boiling tests of four R134a/nanolubricant mixtures with various nanoparticle concentrations in the nanolubricant were made on a horizontal, flat, copper, Turbo-BII-HP-finned surface. A commercial polyolester lubricant (RL68H)[1] with a nominal kinematic viscosity of 72.3 $\mu m^2/s$ at 313.15 K was the base lubricant that was mixed with nominally 10 nm diameter Al_2O_3 nanoparticles. Al_2O_3 nanoparticles have the advantages of a well-established, successful dispersion technology and being relatively inert with respect to lubricated compressor parts.

TEST FLUIDS

A manufacturer used a proprietary surfactant at a mass of 6.2 % of the mass of the Al_2O_3 as a dispersant for the RL68H/Al_2O_3 mixture (nanolubricant). The manufacturer made the mixture such that approximately 24.7 % of the mass was Al_2O_3 particles. From this mixture, nanolubricants with three different mass fractions of Al_2O_3 (5.6 %, 8.2 %, and 16.7 %) were made by adding neat RL68H and ultrasonically mixing the solution for approximately 24 h. The 5.6 %, 8.2 %, and 16.7 % Al_2O_3 mass fractions in the nanolubricant correspond to volume fractions (ϕ) of 1.6 %, 2.3 %, and 5.1 %, respectively. In this study, the 1.6 %, 2.3 %, and 5.1 % volume fraction nanolubricants are identified as 1AlO, 2AlO, and 5AlO, respectively.

Boiling tests with refrigerant/nanolubricant mixtures with increasing concentration of nanoparticles were designed to determine if increases in the nanoparticle surface density of the lubricant excess layer, N_{np}/A_s, resulted in boiling enhancements that agreed with the model introduced in Kedzierski (2012a). The N_{np}/A_s was calculated assuming that all of the nanoparticles charged to the test rig reside uniformly distributed on the heat transfer surface. The test mixtures R134a/1AlO (99.5/0.5), R134a/1AlO (99/1), R134a/2AlO (99/1), and R134a/5AlO (99/1) had nanoparticle surface densities of approximately 2.0×10^{19} m^{-2}, 4.0×10^{19} m^{-2}, 6.8×10^{19} m^{-2}, and 2.8×10^{20} m^{-2}, respectively. The order of magnitude variation in N_{np}/A_s was intended to test the limits of the boiling model. Both the R134a/2AlO and the R134a/5AlO mixtures were tested at only 1 % nanolubricant mass fractions. In addition, the boiling heat transfer of two R134a/RL68H mixtures (0.5 %, and 1 % mass fractions), without nanoparticles, was measured to serve as a baseline for comparison to the nanolubricant mixtures.

APPARATUS

Figure 1 shows a schematic of the apparatus that was used to measure the pool boiling data of this study. More specifically, the apparatus was used to measure the liquid saturation temperature (T_s), the average pool-boiling heat flux (q''), and the wall temperature (T_w) of the test surface. The three principal components of the apparatus were the test chamber, the condenser, and the purger. The internal dimensions of the test chamber were 25.4 mm × 257 mm × 1.54 m. The test chamber was charged with approximately 7 kg of refrigerant, giving a liquid height of approximately 80 mm above the test surface. As shown in Fig. 1, the test section was visible through two opposing, flat 150 mm × 200 mm quartz windows. The bottom of the test surface was heated with high velocity (2.5 m/s) water flow. The vapor produced by liquid boiling on the test surface was condensed by the brine-cooled, shell-and-tube condenser and returned as liquid to the pool by gravity. Further details of the test apparatus can be found in Kedzierski (2002) and Kedzierski (2001b).

TEST SURFACE

Figure 2 shows the oxygen-free high-conductivity (OFHC) copper flat test plate used in this study. The test plate was machined out of a single piece of OFHC copper by electric discharge machining (EDM). The internal fins of a commercial 25 mm (outer-diameter) Turbo-BII-HP tube were removed by EDM. The tube was then cut axially, annealed, flattened, and soldered onto the top of the test plate. Figure 3 shows a photograph of the fin surface. The Turbo-BII-HP has approximately 826 fins per meter (fpm) oriented along the short axis of the plate. The overall height and tip-width of a fin are 0.76 mm and 0.36 mm, respectively.

MEASUREMENTS AND UNCERTAINTIES

The standard uncertainty is the positive square root of the estimated variance. The individual standard uncertainties are combined to obtain the expanded uncertainty (U), which is calculated from the law of propagation of uncertainty with a coverage factor. All measurement uncertainties are reported at the 95 % confidence level except where specified otherwise. For the sake of brevity, only a summary of the basic measurements and uncertainties is given below. Complete detail on the heat transfer measurement techniques and uncertainties can be found in Kedzierski (2000) and Appendix A, respectively.

A Dynamic Light Scattering (DLS) technique was used to measure the average nanoparticle size on a number basis. The diameter of most of the particles (D_{np}) was approximately 10 nm (10.1 nm ± 1.3 nm) and the particles were well dispersed in the lubricant (Kedzierski, 2010). Figure 4 shows a Transmission Electron Microscopy (TEM) image of the nanoparticles as taken by Sarkas (2009). The image confirms the good dispersion and shows that the particles are spherical with most of them having diameters of approximately 10 nm or less and a few having diameters close to 50 nm.

All of the copper-constantan thermocouples and the data acquisition system were calibrated against a glass-rod standard platinum resistance thermometer (SPRT) and a reference voltage to a residual standard deviation of 0.005 K. Considering the fluctuations in the saturation temperature during the test and the standard uncertainties in the calibration, the expanded uncertainty of the average saturation temperature was no greater than 0.04 K. Consequently, it is believed that the expanded uncertainty of the temperature measurements was less than 0.1 K.

Twenty 0.5 mm diameter thermocouples were force fitted into the wells of the side of the test plate shown in Fig. 2. The heat flux and the wall temperature were obtained by regressing the measured temperature distribution of the block to the governing two-dimensional conduction equation (Laplace equation). In other words, rather than using the boundary conditions to solve for the interior temperatures, the interior temperatures were used to solve for the boundary conditions following a backward stepwise procedure given in Kedzierski (1995)[1]. As shown in Fig. 2, the origin of the coordinate system was centered on the surface with respect to the y-direction at the heat transfer surface. Centering the origin in the y-direction reduced the uncertainty of the wall heat flux and temperature calculations by reducing the number of fitted constants involved in these calculations.

Fourier's law and the fitted constants from the Laplace equation were used to calculate the average heat flux (q'') normal to and evaluated at the heat transfer surface based on its projected area. The average wall temperature (T_w) was calculated by integrating the local wall temperature (T). The wall superheat was calculated from T_w and the measured temperature of the saturated liquid (T_s). Considering this, the relative expanded uncertainty in the heat flux ($U_{q''}$) was greatest at the lowest heat fluxes, approaching 13 % of the measurement near 10 kW/m^2. In general, the $U_{q''}$ remained approximately between 3 % and 7 % for heat fluxes greater than 20 kW/m^2. The average random error in the wall superheat (U_{Tw}) remained mainly between 0.06 K and 0.10 K with an average value of approximately 0.07 K. Plots of $U_{q''}$ and U_{Tw} versus heat flux can be found in Appendix A.

EXPERIMENTAL RESULTS

The heat flux was varied between approximately 10 kW/m^2 and 120 kW/m^2 to simulate a range of possible operating conditions for R134a chillers. All pool-boiling measurements were made at 277.6 K saturated conditions. The data were recorded consecutively starting at the largest heat flux and descending in intervals of approximately 4 kW/m^2. The descending heat flux procedure minimized the possibility of any hysteresis effects on the data, which would have made the data sensitive to the initial operating conditions. Table 2 presents the measured heat flux and wall superheat for all the data of this study. Table 3 gives the number of test days and data points for each fluid. A total of 2544 measurements were made over 48 days.

The mixtures were prepared by charging the test chamber (see Fig. 1) with pure R134a to a known mass. Next, a measured mass of nanolubricant or lubricant was injected with a syringe through a port in the test chamber. The refrigerant/lubricant solution was mixed by

[1] Table 1 provides functional forms of the Laplace equation that were used in this study in the same way as was done in Kedzierski (1995) and in similar studies by this author.

flushing pure refrigerant through the same port where the lubricant was injected. All compositions were determined from the masses of the charged components and are given on a mass fraction basis. The maximum uncertainty of the lubricant mass fraction (x_b) measurement is approximately 0.02 %, e.g., the range of a 1.0 % mass fraction is between 0.98 % and 1.02 %. Nominal or target mass compositions are used in the discussion. For example, the "actual" mass composition of the RL68H in the R134a/ RL68H (99.5/0.5) mixture was 0.50 % ± 0.02 %. Likewise, the RL68H mass fraction for the R134a/ RL68H (99/1) mixture was 1.00 % ± 0.02 %. Using the same uncertainties, the nanolubricant mass fractions as tested for R134a/1AlO (99.5/0.5), R134a/1AlO (99/1), R134a/2AlO (99/1), R134a/5AlO (99/1) were 0.50 %, 0.98 %, 1.00 %, and 1.00 %, respectively.

Figure 5 is a plot of the measured heat flux (q") versus the measured wall superheat (T_w - T_s = ΔT_s) for pure R134a pool boiling on the Turbo-BII-HP at a saturation temperature of 277.6 K. These measurements serve as a baseline for comparison to the refrigerant/pure-lubricant measurements. The open triangles represent the measured data while the solid line is a cubic best-fit regression or estimated means of the data. Three days of boiling pure R134a produced 118 measurements over a period of approximately one week. Three of the 118 R134a measurements were removed before fitting because they were identified as "outliers" based on having both high influence and high leverage (Belsley et al., 1980). The data sets for each test fluid presented in this manuscript exhibited a similar number of outliers and were regressed in the same manner. Table 4 gives the constants for the cubic regression of the superheat versus the heat flux for all of the fluids tested here. The residual standard deviation of the regressions – representing the proximity of the data to the mean – are given in Table 5 and are, on average, approximately 0.07 K. The dashed lines to either side of the mean represent the lower and upper 95 % simultaneous (multiple-use) confidence intervals for the mean and are, for the most part, concealed by the data symbols. From the confidence intervals, the expanded uncertainty of the estimated mean wall superheat was, on average, 0.02 K. Table 6 provides the average magnitude of the 95 % multi-use confidence interval for the fitted wall superheat for all of the test data.

Long-dashed lines in Fig. 5 compare pure R134a measurements from two other studies to those of the present study. First, the R134a pool boiling curve of Chen and Tuzla (1996) on a 19 mm OD Turbo-BII-HP tube at T_s = 277.6 K depicted as a dashed line is within 0.4 K of the mean superheat of the present measurements when compared at the same heat flux. Second, the R134a boiling on a Turbo-BII-HP surface taken in the same test apparatus (Kedzierski, 2012b) as the present study is shown as a dashed line that crosses the present measured mean at a superheat of approximately 3.7 K. Overall, the Kedzierski (2012b) boiling curve is within 0.6 K of the mean superheat of the present measurements. It is believed that the above comparisons validate the present measurements.

Figure 6 is a plot of the measured heat flux (q") versus the measured wall superheat (T_w - T_s) for the refrigerant/pure-lubricant mixtures at a saturation temperature of 277.6 K. The refrigerant/pure-lubricant measurements serve as the baseline for comparison to the refrigerant/nanolubricant pool boiling measurements. Thirteen boiling curves were measured over the span of approximately three weeks. The open circles and squares represent the measured heat flux (q") versus the measured wall superheat (T_w - T_s) at a saturation

temperature of 277.6 K for the R134a/RL68H (99.5/0.5) and the R134a/RL68H (99/1) mixtures, respectively. From the 95 % multi-use confidence intervals, the expanded uncertainty of the estimated mean wall superheat was, on average, 0.01 K.

A general overview of the effect that the pure lubricant mass fraction has on R134a/lubricant pool boiling on the Turbo-BII-HP can be obtained from Fig. 6. Comparison of the mean boiling curves for R134a/RL68H (99.5/0.5) and R134a/RL68H (99/1) shows that the superheats are within 0.5 K of each other for the entire tested heat flux with the heat transfer of the (99.5/0.5) mixture being greater than that of the (99/1) mixture for the same superheat. The superheat for the R134a/RL68H (99.5/0.5) mixtures is roughly 0.1 K greater and 0.4 K greater than that for pure R134a at 30 kW/m^2 and 107 kW/m^2, respectively. Addition of lubricant to pure R134a has caused a degradation in the boiling heat transfer of R134a. Kedzierski (2001a) has shown that, in general, degradations associated with increased lubricant mass fractions occur when the concentration-induced bubble size reduction, and its accompanying loss of vapor generation per bubble, is not compensated by an increase in site density. Typically, heat transfer degradations have been observed to increase with respect to increasing lubricant mass fraction. The present measurements are consistent with this heat transfer performance trend where the (99.5/0.5) mixture provides a better boiling performance than that of the (99/1) mixture.

A more precise comparison of the R134a/RL68H heat transfer performances relative to pure R134a is given in Fig. 7. Figure 7 plots the ratio of the R134a/RL68H mixture heat flux to the pure R134a heat flux (q''_{PL}/q''_p) versus the pure R134a heat flux (q''_p) at the same wall superheat. Figure 7 illustrates the influence of lubricant mass fraction on the R134a/RL68H boiling curve with solid and dashed lines representing the mean heat flux ratios for each mixture and shaded regions showing the 95 % multi-use confidence level for each mean. A heat transfer degradation exists where the heat flux ratio is less than one and the 95 % simultaneous confidence intervals (depicted by the shaded regions) do not include the value one. Figure 7 shows that a boiling heat transfer degradation exists for the entire heat flux range for the R134a/RL68H (99/1) mixture. Likewise, the R134a/RL68H (99.5/0.5) exhibits a heat transfer degradation for heat fluxes greater than 40 kW/m^2. For heat fluxes less than 40 kW/m^2, it cannot be stated that the boiling heat transfer for the (99.5/0.5) mixture differs from that of pure R134a. The heat flux ratio is relatively constant but decreased marginally with respect to increasing q''_p. More specifically, the q''_{PL}/q''_p for the (99/1) mixture decreased from approximately 0.89 to 0.83 and that for the (99.5/0.5) mixture decreased from 0.98 to 0.91 for an increase in q''_p from 30 kW/m^2 to110 kW/m^2. The average measured heat flux ratio (q''_{PL}/q''_p), between roughly 30 kW/m^2 and 110 kW/m^2, was approximately 0.95 ± 0.01 and 0.85 ± 0.01 for the (99.5/0.5) and the (99/1) mixture, respectively.

Figure 8 shows the measured heat flux (q'') versus the measured wall superheat (T_w - T_s) for four mixtures of R134a and three different nanolubricants at a saturation temperature of 277.6 K. Thirty-two boiling curves were measured over the span of approximately three months. The closed circles, squares, diamonds, and triangles represent the measurements for the R134a/1AlO (99.5/0.5), R134a/1AlO (99/1), R134a/2AlO (99/1), and R134a/5AlO (99/1) mixtures, respectively. From the 95 % multi-use confidence intervals, the expanded uncertainty of the estimated mean wall superheat was, on average, 0.02 K.

Figure 8 shows three groups of boiling curves with similar heat transfer performance within the group: one for the 1AlO (99/1) and 2AlO (99/1) mixtures, which is in the middle of a group to its left (1AlO, 99.5/0.5) and one to its right (5AlO, 99/1). The boiling curve for the 1AlO (99.5/0.5) mixture exhibits the best heat transfer having a heat flux that is roughly 5 % greater than that for pure R134a and approximately 10 % greater than that for refrigerant/RL68H (99.5/0.5) without nanoparticles (shown in Fig. 6). However, the boiling performance decreases for larger nanoparticle surface density. For example, the boiling curves for the 1AlO (99/1) and 2AlO (99/1) mixtures, having a N_{np}/A_s 95 % larger and 231 % larger than that of 1AlO (99.5/0.5), respectively, have heat fluxes that are approximately 10 % less than that of 1AlO (99.5/0.5) for the same superheat. Further increase in N_{np}/A_s to more than 10 times that of 1AlO (99.5/0.5) resulted in heat fluxes that were roughly 30 % less than that of 1AlO (99.5/0.5).

Figure 9 summarizes the influence of Al_2O_3 nanoparticles on R134a/RL68H boiling heat transfer. The figure plots the ratio of the R134a/RL68H/Al_2O_3 nanoparticles heat flux to the R134a/RL68H heat flux (q''_{Al}/q''_{PL}) versus the R134a/RL68H mixture heat flux (q''_{PL}) at the same wall superheat and lubricant mass fraction for the Turbo-BII-HP. Figure 9 presents the same measurements of the means for the same mixtures that were presented in Fig. 8 as solid lines where each R134a/nanolubricant mixture is compared to the mean of the R134a/pure-lubricant mixture at the same mass fraction. The maximum heat flux ratio for the R134a/1AlO (99.5/0.5) mixture was 1.16 ± 0.02 at a heat flux of 16.5 kW/m^2. The heat flux ratio, for this mixture, averaged from 10 kW/m^2 and 100 kW/m^2 was approximately 1.13. The maximum heat flux ratio for the R134a/1AlO (99/1) mixture was 1.13 ± 0.01 at a heat flux of 33.3 kW/m^2. The heat flux ratio, for this mixture, averaged from 10 kW/m^2 and 100 kW/m^2 was approximately 1.10. The maximum heat flux ratio for the R134a/2AlO (99/1) mixture was 1.11 ± 0.01 at a heat flux of 28.8 kW/m^2. The heat flux ratio, for this mixture, averaged from 10 kW/m^2 and 100 kW/m^2 was approximately 1.09. The maximum heat flux ratio for the R134a/5AlO (99/1) mixture was 0.87 ± 0.02 at a heat flux of 26 kW/m^2. The heat flux ratio, for this mixture, averaged from 10 kW/m^2 and 100 kW/m^2 was approximately 0.86.

DISCUSSION/MODEL DEVELOPMENT

Recall that the purpose of this study was to determine if the performance of reentrant cavity type surfaces could be enhanced with nanolubricants and, if so, would the enhancement follow the refrigerant/nanolubricant boiling theory developed in Kedzierski (2012a). One of the principles of the refrigerant/nanolubricant boiling theory is shown in Fig. 10, taken from Kedzierski (2012a), which illustrates that the absolute number of nanoparticles that are suspended in the lubricant excess layer of the boiling surface is a key determinant for the boiling enhancement. Figure 10 provides the heat flux ratio averaged between a q''_{PL} of 20 kW/m^2 and 40 kW/m^2 as a function of N_{np}/A_s for three different boiling surfaces. Measurements for the present study have been added to Fig. 10 using the star symbol. The point of Fig. 10 is that despite the variation in nanoparticle volume fraction, refrigerant/nanolubricant mass fraction, and the boiling surface geometry, the boiling enhancement follows the general trend of increasing with respect to nanoparticle surface density.

Comparison of the present measurements to the mean of the Fig. 10 data is not entirely conclusive. If only the measurements with the three lowest values of N_{np}/A_s are considered, then the largest deviation from the 95 % confidence interval of the mean is roughly 0.01, while the measurement for the third largest N_{np}/A_s is within the confidence interval. These three data points are neither strong confirmation nor sufficient condemnation of the theory. However, the measurement for the largest N_{np}/A_s is approximately 31 % less than the mean of Fig. 10. This would be supportive evidence to at least begin to question the theory that N_{np}/A_s governs the boiling enhancement had there not been significant nanoparticle agglomeration observed during boiling. Consequently, the heat transfer degradation with respect to increase in N_{np}/A_s, for the case of largest N_{np}/A_s, is attributed to the observed nanoparticle agglomeration. Agglomeration causes loss of nucleation sites by filling the boiling cavities with nanoparticles and in addition, agglomeration prevents the nanoparticles from becoming part of the lubricant excess layer where they interact with bubbles to induce an enhancement (Kedzierski, 2012c). An attempt was made during testing to remedy this by attaching an acoustic transducer to the side of the test chamber above the boiling surface; however, visible agglomerated nanoparticles persisted. As a result, these tests are not adequate to prove or disprove the theory that continued increase in the absolute number of nanoparticles in the nanolubricant improves the boiling.

Equation 1 gives the boiling heat transfer model for refrigerant/aluminum oxide nanolubricant mixtures valid for a plain surface and a rectangular-finned surface as a function of surface geometry dependent nanoparticle surface density; $(N_{np}/A_s)_G$ (Kedzierski, 2012c):

$$\frac{q''_{np}}{q''_{PL}} = 1 + \frac{1.45\times10^{-9}[\mathrm{s\cdot m^{-1}}]\left.\frac{N_{np}}{A_s}\right|_G \sigma \nu_L \rho_v x_b}{D_{np}\left(q''_n\right)^{3/2}\rho_L\left(\rho_{np}-\rho_L\right)g(1-x_b)^2} \tag{1}$$

where q''_n is equal to q''_{PL} normalized by 1 $\mathrm{Wm^{-2}}$. Properties included in eq. (1) are the refrigerant surface tension (σ), the refrigerant vapor density (ρ_v), the neat lubricant liquid density (ρ_L) and liquid kinematic viscosity (ν_L), and the nanoparticle density (ρ_{np}).

The model above is based on the assumption that the enhancement is due to surface work on bubbles as caused by momentum transfer between growing bubbles and nanoparticles suspended within the lubricant excess layer. Equation 1 is a function of the surface geometry dependent nanoparticle surface density: $(N_{np}/A_s)_G$. For the smooth surface, $(N_{np}/A_s)_G$ is equal to N_{np}/A_s. The N_{np}/A_s is obtained by calculating the entire active surface area of the evaporator (A_s) and dividing it into the total number of nanoparticles (N_{np}) charged to the evaporator, which can be obtained by assuming a spherical particle diameter of an average size.

The expression for $(N_{np}/A_s)_G$ that, when substituted into eq. (1), makes it valid for the rectangular fin surface is a function of the normalized pure lubricant heat flux (q''_n) and N_{np}/A_s (Kedzierski, 2012c):

$$\left.\frac{N_{np}}{A_s}\right|_G = 4.15\times10^8\left(q_n^{"}\right)^{2.53}\left(\frac{N_{np}}{A_s}\cdot1\times10^{-20}\right)^{1.47} \quad (2)$$

The leading constant includes the surface geometry effects for the 826 fins per meter (fpm) rectangular-finned surface with overall fin-height and fin-tip-width of 0.76 mm and 0.36 mm, respectively. A crude modification of eq. (2) to make it valid for the 1AlO (99.5/0.5) mixture boiling on the Turbo-BII-HP is done so by adding an additional term to account for the additional surface area of the Turbo-BII-HP and the greater effectiveness of the surface as compared to the rectangular-finned surface:

$$\left.\frac{N_{np}}{A_s}\right|_G = 4.15\times10^8\left(q_n^{"}\right)^{2.53}\left(\frac{N_{np}}{A_s}\cdot1\times10^{-20}\right)^{1.47} + 0.00017q_n^{"} \quad (3)$$

The additional term is a function of the normalized heat flux to account for the increased interaction between bubble and nanoparticles with increase in heat flux as more of the surface becomes active with bubble nucleation. This term was determined from regressing with the measured 1AlO (99.5/0.5) heat flux ratio. The other mixtures were not used in the regression because full dispersion of the nanoparticles was not certain.

Figure 11 shows the predictions of eq. (1) while using the expression for $(N_{np}/A_s)_G$ for the Turbo-BII-HP fin as given by eq. (3). Predictions using eq. (1) together with eq. (3) were done for three of the four refrigerant/nanolubricant mixtures of the study over the entire test heat flux range. The 5AlO (99/1) mixture was not included in the prediction because the nanoparticles were not well dispersed in the lubricant excess layer. For heat fluxes greater than 35 kWm^{-2}, the predictions for the 1AlO (99.5/0.5) mixture are within 0.5 % of the measured means. For heat fluxes less than 35 kWm^{-2}, the 1AlO (99.5/0.5) mixture predictions are on average 4 % greater than the measured means. For heat fluxes greater than 35 kWm^{-2}, the 1AlO (99/1) mixture and the 2AlO (99/1) mixture are overpredicted by, on average, 21 % and 16 %, respectively. It is possible that particle agglomeration may have reduced the nanoparticle surface density contributing to the overprediction of the 1AlO (99/1) and the 2AlO (99/1) mixtures.

Future research is required to devise a method to measure the quality of the nanoparticle dispersion in the lubricant excess layer on a boiling surface. This will permit further improvements on the refrigerant/nanolubricant boiling heat transfer model by qualifying data that is suitable for analysis. Without a reliable means for qualifying the dispersion in the lubricant excess layer, it is not possible to conclusively attribute the boiling heat transfer degradation of the previous study (Kedzierski, 2012b) and that observed in the present to nanoparticle agglomeration. Additional areas for future research are methods for dispersing agglomerated nanoparticles in actively boiling fluids, e.g., acoustic excitation.

CONCLUSIONS

The effect of Al_2O_3 nanoparticles on the boiling performance of R134a/polyolester mixtures on a flattened, horizontal Turbo-BII-HP was investigated. Nanolubricants containing roughly 10 nm diameter Al_2O_3 nanoparticles of various volume fractions with a polyolester lubricant was mixed with R134a at two different mass fractions. The study showed that

nanolubricants can improve R134a boiling on a Turbo-BII-HP, thus demonstrating that the boiling performance of reentrant cavity surfaces can be enhanced if a sufficient nanoparticle surface density is achieved. For example, the R134a/1Al0 (99.5/0.5), R134a/1Al0 (99/1), and the R134a/2Al0 (99/1) mixtures exhibited average enhancement of approximately 13 %, 10 % and 9 %, respectively. Only the R134a/5AlO (99/1) mixture exhibited an average heat transfer degradation of approximately 14 % and this was believed to be due to nanoparticle agglomeration.

An expression for the nanoparticle surface density was developed for the Turbo-BII-HP surface for use in an existing model for predicting refrigerant/nanolubricant boiling. For heat fluxes greater than 35 kWm^{-2}, the model is within 0.5 %, 21 %, and 16 % of the measured heat flux ratios for the 1AlO (99.5/0.5), the 1AlO (99/1), and the 2AlO (99/1) mixtures, respectively. It is possible that particle agglomeration may have reduced the nanoparticle surface density contributing to the deviation of the model from the measurements for the 1AlO (99/1) and the 2AlO (99/1) mixtures. However, without a reliable means for qualifying the dispersion in the lubricant excess layer, it is not possible to conclusively attribute the deviation to nanoparticle agglomeration.

ACKNOWLEDGEMENTS
This work was funded by the U.S. Department of Energy (project no. DE-EE0002057/004) under Project Manager Antonio Bouza. Thanks go to Dongsoo Jung of Inha University and to the following NIST personnel for their constructive criticism of the draft manuscript: A. Pertzborn, and P. Domanski. Furthermore, the author extends appreciation to W. Guthrie and A. Heckert of the NIST Statistical Engineering Division for their consultations on the uncertainty analysis. Boiling heat transfer measurements were taken by D. Wilmering of KT Consulting at the NIST laboratory. The RL68H (EMKARATE RL 68H) was donated by K. Lilje of CPI Engineering Services, Inc. The RL68H1AlO was manufactured by Nanophase Technologies with an aluminum oxide and dispersant in RL68H especially for NIST.

NOMENCLATURE

English Symbols

A_n	regression constant in Table 4 n=0,1,2,3
A_s	heat transfer surface area, m
D_{np}	nanoparticle diameter, m
g	gravitational acceleration, $m \cdot s^{-2}$
N_{np}	the number of nanoparticles
N_{np}/A_s	nanoparticle surface density, m^{-2}
q''	average wall heat flux, $W \cdot m^{-2}$
q''_n	$= \frac{q''_{PL}}{1W \cdot m^{-2}}$
T	temperature, K
T_w	temperature at roughened surface, K
U	expanded uncertainty
X	model terms given in Table 2
x_b	bulk lubricant mass fraction

Greek symbols

ΔT_s	wall superheat: T_w - T_s, K
ν	kinematic viscosity, $m^2 \cdot s^{-1}$
σ	surface tension of refrigerant, $N \cdot m^{-1}$
ρ	density, $kg \cdot m^{-3}$
ϕ	nanoparticle volume fraction

English Subscripts

Al	R134a/nanolubricant mixture
G	surface geometry dependent
L	pure lubricant without nanoparticles
nL	nanolubricant
np	nanoparticle/with nanoparticles
p	pure R134a
PL	refrigerant/pure lubricant (R134a/RL68H) mixture
q"	heat flux
s	saturated state
Tw	wall temperature
v	refrigerant vapor

REFERENCES

Belsley, D. A., Kuh, E., and Welsch, R. E., 1980, Regression Diagnostics: Identifying Influential Data and Sources of Collinearity, New York: Wiley.

Bi, S., Shi, L., and Zhang, L., 2007a, "Performance Study of a Domestic Refrigerator Using R134a/Mineral Oil/Nano-TiO_2 as Working Fluid," *Proceedings of International Conference of Refrigeration*, Beijing, ICRO7-B2-346.

Bi, S., Shi, L., and Zhang, L., 2007b, "Application of Nanoparticles in Domestic Refrigerators," Applied Thermal Engineering, Vol. 28, pp. 1834-1843.

Chen, J., and Tuzla, K., 1996, "Heat Transfer Characteristics of Alternative Refrigerants; Volume 3: Condenser and Evaporator Outside Tube," EPRI TR-106016-V3, project 3412-53, Palo Alto.

Das, S. K., Putra, N., and Roetzel, W., 2003, "Pool Boiling Characteristics of Nano Fluids," Int. J. of Heat and Mass Transfer, Vol. 46, No. 5, pp. 4499-4502.

Hu, H., Peng, H., and Ding, G., 2013,"Nucleat Pool Boiling Heat Transfer Characteristics of Refrigerant/Nanolubricant Mixture with Surfactant," Int. J. Refrigeration, Vol. 36, pp. 1045-1055.

Henderson, K., Park, Y., Liu, L., Jacobi, A. M., 2010, "Flow-Boiling Heat Transfer of R-134a-Based Nanofluids in a Horizontal Tube," IJHMT, 53, 944-951

Kedzierski, M. A., 2012a, "R134a/Al2O3 Nanolubricant Mixture Boiling on a Rectangular Finned Surface," ASME J. Heat Transfer, Vol. 134, 121501.

Kedzierski, M. A., 2012b, "Effect of Al_2O_3 Nanolubricant on a Turbo-BII R134a Pool Boiling Surface," *Proceedings of MNHMT2012 3rd Micro/Nanoscale Heat & Mass Transfer International Conference*, Atlanta, Georgia, MNHMT2012-75024.

Kedzierski, M. A., 2012c, "Effect of Diamond Nanolubricant on R134a Pool Boiling Heat Transfer," ASME Journal of Heat Transfer, Vol. 134, 051001.

Kedzierski, M. A., 2011, "Effect of Al_2O_3 Nanolubricant on R134a Pool Boiling Heat Transfer," Int. J. Refrigeration, Vol. 34, pp. 498-508.

Kedzierski, M. A., 2010, "Effect of Al_2O_3 Nanolubricant on a Passively Enhanced R134a Pool Boiling Surface with Extensive Measurement and Analysis Details," NIST Technical Note 1677, U.S. Department of Commerce, Washington, D.C.

Kedzierski, M. A., 2009, "Effect of CuO Nanoparticle Concentration on R134a/Lubricant Pool-Boiling Heat Transfer," ASME J. Heat Transfer, Vol. 131, No. 4, 043205.

Kedzierski, M. A., 2002, "Use of Fluorescence to Measure the Lubricant Excess Surface Density During Pool Boiling," Int. J. Refrigeration, Vol. 25, pp. 1110-1122.

Kedzierski, M. A., 2001a, "The Effect of Lubricant Concentration, Miscibility and Viscosity on R134a Pool Boiling" Int. J. Refrigeration, Vol. 24, No. 4., pp. 348-366.

Kedzierski, M. A., 2001b, "Use of Fluorescence to Measure the Lubricant Excess Surface Density During Pool Boiling," NISTIR 6727, U.S. Department of Commerce, Washington, D.C.

Kedzierski, M. A., 2000, "Enhancement of R123 Pool Boiling by the Addition of Hydrocarbons," Int. J. Refrigeration, Vol. 23, pp. 89-100.

Kedzierski, M. A., 1995, "Calorimetric and Visual Measurements of R123 Pool Boiling on Four Enhanced Surfaces," NISTIR 5732, U.S. Department of Commerce, Washington.

Lee, J, Cho, S., Hwang, Y., Cho, H., J., Lee, C., Choi, Y., Ku, B. C., Lee, H., Lee, B., Kim, B., and Kim, S. H., 2009, "Application of Fullerene-Added Nano-Oil for Lubrication Enhancement in Friction Surfaces," Tribology Int., Vol. 42, pp. 440-447.

Park, K. J., and Jung, D., 2007, "Enhancement of Nucleate Boiling Heat Transfer Using Carbon Nanotubes," Int. J. of Heat and Mass Transfer, Vol. 50, pp. 4499–4502.

Peng, H., Ding, G., Hu, H., and Jiang, W., 2011, "Effect of Nanoparticle Size on Nucleate Pool Boiling Heat Transfer of Refrigerant/oil Mixture with Nanopartilces," Int. J. Heat and Mass Transfer, Vol. 54, pp. 1839-1850.

Peng, H., Ding, G., Hu, H., Jiang, W., Zhuang, D., and Wang, K., 2010, "Nucleate Pool Boiling Heat Transfer Characteristics of Refrigerant/oil Mixture with Diamond Nanopartilces," Int. J. Refrigeration, Vol. 33, pp. 347-358.

Wu, X. M., Li, P., Li, H., Wang, W. C., 2008, "Investigation of Pool Boiling Heat Tranfer of R11 with TiO2 Nano-Particles," J. of Engr. Thermophysics, Vol. 29, No. 1, pp. 124-126.

Sarkas, H., 2009, Private Communications, Nanophase Technologies Corporation, Romeoville, IL.

Trisaksri, V., and Wongwises, S, 2009, "Nucleate Pool Boiling Heat Transfer of T_iO_2-R141b Nanofluids," Int. J. of Heat and Mass Transfer, Vol. 52, No. 5-6, pp. 1582-1588.

Table 1 Conduction model choice

X_0= constant (all models) X_1= x X_2= y X_3= xy $X_4=x^2-y^2$ $X_5= y(3x^2-y^2)$ $X_6= x(3y^2-x^2)$ $X_7= x^4+y^4-6(x^2)y^2$ $X_8= yx^3-xy^3$	
Fluid	Most frequent models
Pure R134a (file: TBC134a.dat)	X_1,X_2,X_5 (78 of 118) 66 % X_1,X_3 (35 of 118) 30 % X_1,X_2,X_3 (5 of 118) 4 %
R134a/RL68H (99.5/0.5) (file:TBCRL5.dat)	X_1,X_2,X_5 (212 of 212) 100 %
R134a/RL68H (99/1) (file: TBCRL1.dat)	X_1,X_2,X_5 (183 of 359) 51 % X_1,X_3(176 of 359) 49 %
R134a/1AlO (99.5/0.5) (file:TBCAL5.dat)	X_1,X_2,X_5 (197 of 402) 49 % X_1,X_3 (143 of 402) 36 % X_1,X_2,X_5,X_7 (5 of 402) 1 %
R134a/1AlO (99/1) (file:TBCAL1.dat)	X_1,X_3 (215 of 420) 51 % X_1,X_2,X_5 (207 of 420) 49 %
R134a/2AlO (99/1) (file:TBCAL81.dat)	X_1,X_3 (403 of 749) 54 % X_1,X_2,X_5 (320 of 749) 43 % X_1,X_2,X_5,X_6 (14 of 749) 2 % X_1,X_2,X_5,X_7 (6 of 749) 1 %
R134a/5AlO (99/1) (file:TBCAL17.dat)	X_1,X_3 (169 of 284) 59 % X_1,X_3,X_5 (86 of 284) 30 % X_1,X_2,X_3 (13 of 284) 5 % X_1, X_5 (9 of 284) 3 %

Table 2 Pool boiling data

Pure R134a
File: TBC134a.dat

ΔT_s (K)	q'' (W/m^2)
5.47	113890.
5.45	113469.
5.45	113573.
5.07	104758.
5.04	104284.
5.03	104384.
4.79	98357.
4.79	98549.
4.78	98543.
4.51	92472.
4.52	92483.
4.50	92444.
4.25	86906.
4.22	86515.
4.21	86056.
3.89	79357.
3.89	79362.
3.88	79346.
3.61	73831.
3.61	73786.
3.61	73674.
3.33	67806.
3.32	67511.
3.31	67515.
3.01	61569.
3.00	61581.
3.01	61533.
2.72	56030.
2.71	56071.
4.87	107861.
4.87	108085.
4.89	108259.
4.66	101618.
4.66	101654.
4.66	101616.
4.43	95485.
4.42	95600.
4.43	95632.
4.20	89740.
4.20	89792.
4.20	89814.
3.97	83809.
3.96	83730.
3.96	83961.
3.72	78183.
3.71	78004.
3.71	77833.
3.47	72487.
3.47	72676.
3.48	72516.
3.20	66597.
3.21	66634.
3.20	66627.
2.95	61231.
2.95	61327.
2.96	61430.
2.71	56023.
2.71	56165.
2.71	56124.
2.44	50586.
2.45	50535.
2.44	50516.
2.18	45849.
2.18	45896.
2.19	45915.
1.95	40610.
1.94	40427.
1.94	40434.
1.70	36158.
1.70	36151.
1.71	36131.
1.50	31930.
1.50	31873.
4.91	107889.
4.94	108234.
4.94	108065.
4.74	101100.
4.75	101029.
4.73	100946.
4.54	94962.
4.54	95017.
4.54	95106.
4.33	88860.
4.32	88948.
4.32	88881.
4.10	82930.
4.10	83246.
4.10	83385.
3.87	76934.
3.86	77002.
3.85	77039.
3.63	71510.
3.63	71586.
3.63	71657.
3.39	65868.
3.37	65929.
3.38	65997.
3.14	60284.
3.13	60223.
3.12	60088.
2.87	55065.
2.88	55120.
2.87	55190.
2.62	49935.
2.61	50000.
2.63	50165.
2.36	44966.
2.35	45047.
2.36	45187.
2.11	39795.
2.09	39894.
2.10	39937.
1.85	35629.
1.86	35656.
1.86	35670.
1.63	31114.
1.62	31189.
1.62	31336.

R134a/RL68H (99.5/0.5)
File: TBCRL5.dat

ΔT_s (K)	q'' (W/m^2)
5.61	110211.
5.60	110303.
5.59	110288.
5.30	104266.
5.31	104294.
5.30	104360.
5.03	98862.
5.03	98970.
5.03	99076.
4.73	92785.
4.73	92930.
4.74	93036.
4.46	87238.
4.46	87251.
4.45	87327.
4.16	81376.
4.16	81459.
4.16	81582.
3.88	75951.
3.87	75959.
3.88	76016.
3.61	70214.
3.61	70277.
3.59	70162.
3.33	64984.
3.33	65095.
3.34	65161.
3.07	59592.
3.06	59566.
3.06	59540.
2.78	53941.
2.78	53968.
2.77	53912.
2.52	48599.
2.52	48596.
2.51	48491.
2.23	43456.
2.24	43477.
5.60	110597.
5.59	110287.
5.58	110300.
5.29	104045.
5.29	104131.
5.30	104271.
5.04	98773.
5.03	98589.
5.04	98600.
4.75	92634.
4.74	92648.
4.74	92658.
4.46	86981.
4.46	87112.
4.47	87101.
4.17	80958.
4.17	80941.
4.16	80931.
3.90	75410.
3.90	75484.
3.90	75557.

3.62	69911.
3.63	69990.
3.62	70047.
3.35	64444.
3.35	64376.
3.35	64272.
3.07	58812.
3.07	58930.
3.07	59011.
2.82	53698.
2.81	53636.
2.81	53665.
2.54	48399.
2.54	48391.
2.55	48442.
2.27	42990.
2.26	42945.
2.26	42947.
1.98	38367.
1.99	38328.
1.99	38377.
1.75	34065.
1.75	33963.
5.51	110725.
5.50	110884.
5.51	110995.
5.22	104593.
5.23	104747.
5.23	104820.
4.95	98624.
4.96	98811.
4.96	98822.
4.69	92809.
4.68	92838.
4.68	92799.
4.41	86946.
4.42	86956.
4.41	87031.
4.14	81560.
4.14	81649.
4.16	81959.
3.89	75757.
3.87	75765.
3.88	75696.
3.61	70035.
3.61	70103.
3.60	70075.
3.34	64531.
3.34	64558.
3.34	64546.
3.07	59076.
3.07	59122.
3.07	59114.
2.79	53640.
2.78	53524.
2.79	53671.
2.53	48396.
2.53	48417.
2.54	48434.
2.26	43234.
2.25	43141.
2.26	43205.
1.99	38444.
1.99	38351.
1.99	38384.

1.75	33996.
1.74	33919.
5.50	111168.
5.51	111350.
5.52	110988.
5.22	104612.
5.23	104758.
5.23	104761.
4.96	98676.
4.96	98643.
4.97	98675.
4.70	92915.
4.69	93003.
4.70	93038.
4.42	86873.
4.42	86933.
4.42	86934.
4.14	81343.
4.14	81457.
4.15	81360.
3.87	76301.
3.88	75909.
3.88	75640.
3.59	70343.
3.60	70376.
3.60	70466.
3.33	64626.
3.33	64651.
3.33	64558.
3.07	59346.
3.07	59399.
3.08	59439.
2.80	53636.
2.79	53628.
2.79	53521.
2.53	48597.
2.53	48714.
2.53	48636.
2.26	43213.
2.26	43281.
2.27	43451.
1.98	38385.
1.98	38437.
1.98	38362.
1.75	33968.
1.73	33814.
5.47	110181.
5.46	110199.
5.47	110247.
5.17	103591.
5.17	103608.
5.16	103567.
4.89	98019.
4.89	98183.
4.91	98322.
4.65	92600.
4.64	92398.
4.64	92226.
4.36	86604.
4.37	86706.
4.36	86820.
4.09	80756.
4.08	80779.
4.09	80784.
3.82	75149.

3.83	75168.
3.82	75159.
3.56	69664.
3.56	69725.
3.57	69806.
3.30	64265.
3.30	64287.
3.29	64331.
3.03	58838.
3.03	58761.
3.03	58791.
2.77	53238.
2.72	53827.
2.73	53870.
2.48	48421.
2.48	48465.
2.48	48534.
2.22	43039.
2.22	43016.
2.21	42790.
1.92	38524.
1.97	37903.
1.92	39081.

R134a/RL68H (99/1)
File: TBCRL1.dat

ΔT_s (K)	q'' (W/m^2)
6.06	109296.
6.02	109216.
6.02	109132.
5.75	103148.
5.75	103276.
5.75	103308.
5.48	97240.
5.32	97963.
5.34	98178.
5.08	92496.
5.08	92507.
5.09	92485.
4.79	86756.
4.79	86589.
4.80	86703.
4.55	81412.
4.55	81508.
4.54	81249.
4.25	75239.
4.24	75157.
4.24	75093.
3.92	69159.
3.92	69231.
3.92	69578.
3.65	64214.
3.66	63966.
5.89	108675.
5.89	108818.
5.89	108944.
5.60	102414.
5.59	102495.
5.59	102803.
5.29	96926.
5.30	97271.

5.31	97271.
5.06	91614.
5.06	91754.
5.06	91801.
4.73	85760.
4.73	85825.
4.75	85878.
4.45	80346.
4.43	80542.
4.49	80703.
4.19	74626.
4.20	74584.
4.20	74689.
3.92	69334.
3.91	69414.
3.92	69450.
3.63	63464.
3.60	63382.
3.60	63449.
3.34	58161.
3.33	58167.
3.33	58048.
3.05	53132.
3.04	53121.
3.04	53284.
2.76	47992.
2.76	47959.
2.76	47980.
2.47	42935.
2.46	43227.
2.46	43271.
2.21	38490.
2.20	38236.
2.20	38178.
1.92	33688.
1.91	33692.
5.89	108513.
5.90	108593.
5.90	108727.
5.62	102274.
5.61	102472.
5.61	102538.
5.34	96444.
5.33	96392.
5.33	96345.
5.05	90570.
5.05	90702.
5.05	90658.
4.79	85394.
4.80	85548.
4.79	85574.
4.48	79470.
4.50	79955.
4.50	79898.
4.22	74126.
4.21	74320.
4.22	74496.
3.93	68678.
3.93	68763.
3.92	68714.
3.66	63409.
3.66	63478.
3.65	63566.
3.36	57893.
3.35	58089.

3.37	58197.
3.09	53110.
3.09	53092.
3.09	53107.
2.80	47761.
2.79	47841.
2.81	47810.
2.53	43325.
2.51	43171.
2.51	43309.
2.25	38588.
2.24	38393.
2.23	38374.
1.96	33624.
1.94	33495.
1.95	33660.
1.70	29535.
1.69	29389.
5.90	108940.
5.90	109137.
5.90	109202.
5.60	102375.
5.59	102345.
5.59	102528.
5.32	97015.
5.32	97111.
5.32	97226.
5.05	91224.
5.05	91334.
5.04	91200.
4.76	85441.
4.77	85804.
4.78	85885.
4.47	79757.
4.47	79702.
4.47	79654.
4.20	74673.
4.21	74701.
4.21	74686.
3.92	68971.
3.91	69009.
3.91	68998.
3.63	63484.
3.62	63519.
3.62	63416.
3.34	58444.
3.34	58481.
3.35	58629.
3.08	53286.
3.07	53197.
3.07	53183.
2.79	48255.
2.80	48296.
2.80	48189.
2.51	43255.
2.50	43369.
2.51	43377.
2.24	38337.
2.22	38313.
2.22	38296.
1.95	33944.
1.94	33832.
1.94	33803.
1.69	29416.
1.68	29260.

5.95	109349.
5.96	109576.
5.96	109619.
5.66	103050.
5.66	103048.
5.67	103134.
5.40	97441.
5.40	97531.
5.40	97344.
5.12	91685.
5.12	91660.
5.12	91782.
4.84	85984.
4.84	86109.
4.84	85839.
4.55	80268.
4.55	80523.
4.56	80488.
4.26	74635.
4.26	74388.
4.26	74480.
3.98	69325.
3.99	69505.
3.98	69478.
3.71	63977.
3.70	63887.
3.70	63734.
3.41	58650.
3.42	58749.
3.41	58692.
3.14	53235.
3.12	53134.
3.12	53074.
2.84	48363.
2.85	48471.
2.85	48454.
2.57	43700.
2.56	43604.
2.56	43605.
2.29	38718.
2.27	38710.
2.27	38711.
2.00	34149.
1.98	33937.
5.93	109447.
5.94	109746.
5.93	109816.
5.64	102930.
5.65	103020.
5.64	103242.
5.37	97252.
5.37	97295.
5.37	97441.
5.10	91649.
5.10	91784.
5.10	91665.
4.83	86060.
4.82	85953.
4.82	85967.
4.53	80167.
4.53	79977.
4.53	80076.
4.24	74495.
4.23	74579.
4.24	74642.

3.97	68987.
3.96	69108.
3.96	69197.
3.69	63877.
3.69	63943.
3.70	64009.
3.40	58251.
3.40	58466.
3.40	58476.
3.12	53253.
3.12	53203.
3.11	53148.
2.84	48345.
2.84	48586.
2.85	48324.
2.56	43291.
2.54	43300.
2.54	43329.
2.27	38442.
2.24	38158.
2.23	38101.
1.95	33637.
1.94	33697.
5.38	96378.
5.38	96278.
5.38	96419.
5.11	90746.
5.11	90882.
5.12	90936.
4.84	85142.
4.83	85034.
4.84	85150.
4.54	79220.
4.54	79187.
4.54	79279.
4.25	74205.
4.27	74315.
4.27	74381.
3.98	68783.
3.98	68777.
3.98	68712.
3.70	63182.
3.67	63121.
3.68	62891.
3.40	58100.
3.40	57958.
3.41	57913.
3.11	53076.
3.10	52870.
3.09	52769.
2.81	47810.
2.80	47871.
2.80	47686.
2.52	42863.
2.50	42539.
2.49	42518.
2.23	38108.
2.22	38186.
2.22	38094.
1.95	33707.
1.95	33644.
1.95	33862.
1.68	29475.
1.67	29107.
1.68	29374.

1.46	25337.
1.43	25033.
1.43	24833.
1.20	21595.
1.15	21212.
1.15	21094.
0.92	17477.
0.89	17044.
0.88	16898.
0.62	13450.
0.59	13245.
5.31	96522.
5.31	96861.
5.31	96974.
5.04	90821.
5.04	90905.
5.04	91033.
4.74	85093.
4.74	85058.
4.74	85090.
4.45	79237.
4.46	79275.
4.46	79514.
4.18	73811.
4.18	73811.
4.18	73997.
3.91	68310.
3.88	68381.
3.91	68361.
3.60	62903.
3.59	62972.
3.60	63082.
3.28	57931.
3.26	58060.
3.25	58003.
3.02	52771.
3.04	52815.
3.03	52816.
2.75	48045.
2.72	48093.
2.76	48016.
2.47	42868.
2.45	42809.
2.44	42832.
2.24	38186.
2.23	38140.
2.25	38188.
2.00	33702.
1.99	33697.
1.99	33490.
1.72	29492.
1.70	29444.
1.71	29377.
1.47	25269.
1.46	24893.
1.46	25082.
1.22	21142.
1.20	20831.
1.20	20838.
0.94	17449.
0.91	16802.
0.90	16777.
0.67	13435.
0.67	13454.
0.67	13319.

R134a/1ALO (99.5/0.5)
File: TBCAL5.dat

ΔT_s (K)	q'' (W/m^2)
5.24	112950.
5.25	113082.
5.26	112719.
5.00	106344.
5.01	106490.
5.02	106595.
4.76	100085.
4.76	100379.
4.77	100060.
4.49	93887.
4.48	93916.
4.48	94102.
4.23	88118.
4.22	88124.
4.22	88287.
3.97	82391.
3.97	82412.
3.97	82395.
3.68	76695.
3.69	76746.
3.68	76776.
3.42	71525.
3.42	71641.
3.43	71588.
3.18	66145.
3.18	66158.
3.18	66092.
2.93	60792.
2.92	60685.
2.91	60654.
2.67	55431.
2.66	55479.
2.65	55339.
2.42	50461.
2.42	50260.
2.40	50082.
2.16	45068.
2.15	44934.
2.15	44982.
1.91	40256.
1.89	40070.
1.91	40155.
1.65	35261.
1.65	35198.
1.65	35130.
1.42	30934.
1.40	30753.
1.41	30674.
1.18	26240.
1.18	25891.
1.17	25773.
0.96	21924.
0.94	21648.
0.94	21525.
0.73	17657.
0.71	17379.
5.36	111708.

5.36	111580.
5.35	111585.
5.07	104957.
5.07	105153.
5.09	105243.
4.81	99180.
4.82	99634.
4.83	99562.
4.55	93443.
4.56	93625.
4.56	93576.
4.27	87870.
4.27	87973.
4.27	88045.
3.99	82231.
3.98	82382.
3.99	82393.
3.72	76821.
3.72	76811.
3.72	76844.
3.45	71305.
3.44	71271.
3.44	71434.
3.18	65916.
3.17	66016.
3.18	66144.
2.93	60556.
2.92	60420.
2.92	60413.
2.65	55363.
2.65	55276.
2.65	55251.
2.39	50173.
2.39	50001.
2.38	50061.
2.15	45507.
2.15	45395.
2.15	45193.
1.90	40090.
1.89	39926.
1.89	39858.
1.63	35018.
1.62	34934.
1.62	34970.
1.39	30882.
1.40	30827.
1.40	30822.
1.16	26290.
1.16	25956.
1.15	25911.
0.95	22094.
0.92	21689.
0.92	21621.
0.71	17607.
0.68	17231.
5.23	112163.
5.23	112418.
5.23	112412.
4.96	106133.
4.97	106247.
4.96	106267.
4.68	99913.
4.68	99879.
4.68	100030.
4.40	94157.
4.39	94182.
4.41	94292.
4.13	87926.
4.13	88032.
4.13	87811.
3.83	81978.
3.82	81943.
3.82	82076.
3.54	76454.
3.54	76753.
3.55	76977.
3.30	71199.
3.30	71279.
3.30	71248.
3.05	65899.
3.04	65798.
3.04	65711.
2.81	60334.
2.81	60518.
2.81	60492.
2.56	54983.
2.56	55042.
2.56	55018.
2.32	50257.
2.31	50222.
2.31	49979.
2.08	45181.
2.08	44950.
2.08	45050.
1.85	40408.
1.85	39984.
1.84	40061.
1.58	35069.
1.58	35030.
1.58	34865.
1.35	30558.
1.34	30444.
1.35	30356.
1.13	25888.
1.11	25820.
1.11	25630.
0.90	21395.
0.89	21156.
0.89	21076.
0.66	16974.
0.66	17090.
0.66	16980.
0.49	13177.
0.48	13099.
5.16	112641.
5.16	112652.
5.16	112728.
4.85	105831.
4.85	106161.
4.85	106190.
4.59	100438.
4.59	100556.
4.62	100541.
4.34	94220.
4.35	94095.
4.36	94479.
4.09	88517.
4.09	88688.
4.09	88737.
3.80	82797.
3.81	83177.
3.81	83343.
3.52	77297.
3.52	77898.
3.54	77606.
3.28	72256.
3.29	72034.
3.30	72097.
3.03	66851.
3.03	66749.
3.03	66936.
2.79	61452.
2.78	61198.
2.78	61118.
2.53	56104.
2.52	56127.
2.52	56236.
2.27	50995.
2.27	50728.
2.27	50778.
2.07	45733.
2.06	45497.
2.06	45437.
1.81	40641.
1.80	40706.
1.80	40575.
1.56	35634.
1.57	35484.
1.56	35404.
1.35	31141.
1.35	30862.
1.35	30821.
1.12	26359.
1.11	25977.
1.10	26067.
0.90	22023.
0.88	21811.
0.88	21816.
0.68	17885.
0.66	17578.
0.66	17542.
0.47	13354.
0.47	13231.
5.07	112580.
5.07	112663.
5.07	112818.
4.81	106509.
4.80	106616.
4.80	106912.
4.53	100410.
4.51	100531.
4.51	100610.
4.24	94491.
4.24	94649.
4.24	94651.
3.99	88749.
4.00	88620.
3.99	88877.
3.72	83071.
3.73	82850.
3.74	83056.
3.48	77524.
3.49	77806.
3.51	77711.
3.25	71793.

3.26	71990.
3.26	72043.
3.02	66587.
3.01	66696.
3.01	66741.
2.75	61184.
2.75	61248.
2.75	61244.
2.51	55943.
2.49	56089.
2.50	56029.
2.26	50753.
2.26	50533.
2.27	50353.
2.03	45796.
2.03	45740.
2.04	45827.
1.81	40463.
1.79	40360.
1.80	40159.
1.56	35388.
1.54	35298.
1.54	35332.
1.33	30823.
1.33	30792.
1.33	30762.
1.12	26308.
1.09	26160.
1.09	26034.
0.89	22047.
0.87	21919.
0.88	21860.
0.69	17565.
0.66	17128.
0.66	16982.
0.47	13295.
0.46	13295.
5.05	112931.
5.06	112570.
5.07	112632.
4.81	106690.
4.82	106874.
4.81	106735.
4.53	100591.
4.54	100662.
4.54	100788.
4.27	94735.
4.25	94753.
4.26	94881.
3.99	88864.
3.99	88978.
3.99	88963.
3.72	82454.
3.74	82692.
3.73	82687.
3.47	77205.
3.47	77248.
3.46	77210.
3.22	71685.
3.21	71503.
3.23	71599.
2.97	66544.
2.96	66379.
2.97	66192.
2.71	60949.

2.72	61060.
2.72	61017.
2.47	55871.
2.47	55809.
2.47	55871.
2.24	50656.
2.23	50486.
2.22	50460.
1.99	45418.
1.99	45635.
2.00	45752.
1.78	40505.
1.78	40406.
1.77	40445.
1.53	35249.
1.53	35024.
1.53	35056.
1.31	30671.
1.30	30453.
1.30	30394.
1.09	26181.
1.08	25889.
1.08	25873.
0.88	21763.
0.87	21681.
0.88	21656.
0.68	17447.
0.68	17246.
0.68	17177.
0.49	13285.
0.47	13217.
5.08	112508.
5.09	112788.
5.10	112540.
4.82	106262.
4.81	106456.
4.82	106619.
4.55	100402.
4.55	100376.
4.56	100228.
4.27	94606.
4.28	94567.
4.31	94840.
4.03	88810.
4.03	88850.
4.02	89012.
3.74	82740.
3.74	82748.
3.74	82893.
3.48	77361.
3.47	77428.
3.48	77308.
3.21	71833.
3.20	71971.
3.21	72048.
2.96	66765.
2.97	66810.
2.96	66680.
2.71	61818.
2.72	61526.
2.72	61488.
2.45	55716.
2.45	55958.
2.45	55888.
2.19	50663.

2.19	50565.
2.19	50444.
1.99	45898.
1.98	45619.
1.98	45664.
1.76	40647.
1.76	40519.
1.76	40406.
1.52	35419.
1.52	35132.
1.52	35085.
1.30	30841.
1.29	30801.
1.31	30646.
1.07	26323.
1.06	26007.
1.06	25980.
0.86	21936.
0.86	21810.
0.85	21825.

R134a/1Al0 (99/1)
File: RFAl5.dat

ΔT_s (K)	q'' (W/m^2)
5.90	110502.
5.89	110450.
5.90	110621.
5.62	105016.
5.62	105149.
5.63	105259.
5.34	99359.
5.35	99453.
5.35	99417.
5.05	93478.
5.06	93498.
5.06	93605.
4.76	87958.
4.76	88128.
4.77	88093.
4.45	82156.
4.46	82219.
4.45	82108.
4.12	76405.
4.12	76591.
4.13	76702.
3.82	71015.
3.81	70909.
3.81	71028.
3.51	65763.
3.51	65662.
3.52	65855.
3.22	60432.
3.22	60280.
3.23	60247.
2.94	55154.
2.95	55222.
2.95	55118.
2.68	50321.
2.68	50368.

2.68	50352.
2.41	45139.
2.40	45067.
2.40	44910.
2.14	40315.
2.14	40174.
2.14	40093.
1.88	35219.
1.87	35234.
1.88	35151.
1.62	30734.
1.63	30721.
1.63	30632.
1.40	26418.
1.37	25880.
1.38	26012.
1.13	22045.
1.11	21821.
1.11	21798.
0.90	17851.
0.88	17562.
0.88	17544.
0.66	13711.
0.63	13237.
0.62	13099.
0.46	10625.
0.39	9768.
5.68	109447.
5.69	110492.
5.71	110591.
5.42	104581.
5.44	104848.
5.47	104204.
5.22	99194.
5.23	99094.
5.24	99380.
4.94	93738.
4.95	93783.
4.96	93760.
4.64	87724.
4.64	87858.
4.64	87824.
4.32	81953.
4.32	82101.
4.32	82086.
4.01	76490.
4.01	76647.
4.02	76611.
3.72	70794.
3.71	70652.
3.72	70675.
3.43	65531.
3.43	65661.
3.44	65723.
3.17	60162.
3.16	60095.
3.16	60035.
2.88	55019.
2.88	55164.
2.88	55080.
2.64	50285.
2.63	50174.
2.63	50059.
2.37	45198.
2.37	45208.

2.37	45180.
2.11	40216.
2.10	39977.
2.10	40028.
1.85	35513.
1.84	35343.
1.84	35451.
1.59	30808.
1.59	30709.
1.60	30517.
1.36	26572.
1.35	26347.
1.34	26134.
1.09	21967.
1.08	21741.
1.07	21716.
0.87	17789.
0.85	17369.
0.85	17256.
0.61	13593.
0.59	13435.
5.58	110468.
5.59	110516.
5.59	110492.
5.34	104572.
5.37	104793.
5.43	104249.
5.14	99488.
5.16	99527.
5.15	99662.
4.86	93618.
4.86	93631.
4.86	93758.
4.56	87944.
4.56	88014.
4.57	88065.
4.25	81817.
4.24	81802.
4.25	81964.
3.94	76368.
3.93	76367.
3.95	76501.
3.66	71022.
3.65	70995.
3.65	71086.
3.38	65457.
3.38	65611.
3.37	65498.
3.10	60278.
3.10	60328.
3.10	60360.
2.84	55012.
2.84	54979.
2.82	54917.
2.58	50058.
2.57	50019.
2.57	50060.
2.32	45302.
2.31	45371.
2.32	45307.
2.08	40440.
2.08	40205.
2.09	40095.
1.81	35277.
1.80	35232.

1.78	35245.
1.54	30579.
1.54	30374.
1.55	30298.
1.32	26294.
1.31	26138.
1.31	26191.
1.09	21579.
1.05	21370.
1.05	21316.
0.84	17527.
0.81	17254.
0.81	17119.
0.59	13812.
0.57	13391.
5.57	110368.
5.58	110631.
5.59	111052.
5.32	104194.
5.32	104437.
5.35	104637.
5.06	98766.
5.07	98865.
5.07	99053.
4.79	93240.
4.79	93235.
4.80	93535.
4.51	87631.
4.51	87745.
4.52	87864.
4.20	81906.
4.21	82125.
4.20	82041.
3.92	76088.
3.93	76360.
3.93	76228.
3.63	70904.
3.64	70895.
3.64	70659.
3.35	65280.
3.35	65330.
3.36	65314.
3.09	60135.
3.09	60283.
3.10	60362.
2.86	55310.
2.85	55190.
2.86	55236.
2.60	50287.
2.59	50269.
2.60	50225.
2.34	45240.
2.34	45188.
2.34	45239.
2.09	40465.
2.09	40267.
2.07	40201.
1.83	35257.
1.81	34941.
1.81	34977.
1.57	30547.
1.57	30374.
1.57	30443.
1.34	26409.
1.34	26194.

1.33	26187.
1.09	21848.
1.07	21644.
1.08	21581.
0.86	17897.
0.84	17490.
0.83	17344.
0.61	13607.
0.60	13388.
5.55	110539.
5.57	110647.
5.60	109672.
5.34	105082.
5.35	105206.
5.37	105276.
5.08	99514.
5.09	99455.
5.10	99510.
4.81	93545.
4.80	93596.
4.81	93725.
4.52	88080.
4.51	88196.
4.53	88142.
4.21	82053.
4.21	82153.
4.21	82082.
3.92	76488.
3.91	76587.
3.92	76608.
3.63	70995.
3.62	71050.
3.62	71096.
3.34	65475.
3.34	65619.
3.35	65637.
3.07	60223.
3.07	60235.
3.07	60277.
2.81	55065.
2.81	55002.
2.81	54849.
2.56	50416.
2.56	50401.
2.56	50399.
2.31	45259.
2.31	45212.
2.30	45243.
2.06	40234.
2.05	40200.
2.05	40178.
1.78	35178.
1.77	35146.
1.77	35084.
1.51	30406.
1.52	30530.
1.51	30236.
1.30	26208.
1.30	26089.
1.31	26223.
1.07	21781.
1.06	21709.
1.07	21679.
0.86	18022.
0.83	17574.

0.82	17505.
0.60	13538.
0.58	13243.
5.51	110614.
5.52	110776.
5.54	110830.
5.27	104484.
5.30	104683.
5.30	104707.
5.04	99420.
5.04	99276.
5.05	99220.
4.77	93696.
4.76	93747.
4.78	93880.
4.48	87871.
4.49	87946.
4.50	88061.
4.18	82043.
4.18	81999.
4.18	82137.
3.88	76362.
3.89	76451.
3.90	76659.
3.62	71141.
3.63	71227.
3.63	71332.
3.36	65680.
3.36	65691.
3.36	65758.
3.07	60478.
3.07	60436.
3.09	60599.
2.82	55386.
2.83	55465.
2.83	55470.
2.58	50428.
2.56	50461.
2.56	50467.
2.31	45475.
2.31	45313.
2.31	45315.
2.06	40233.
2.04	40053.
2.04	39979.
1.78	35397.
1.76	35151.
1.76	35242.
1.53	30726.
1.52	30610.
1.53	30728.
1.31	26604.
1.29	26183.
1.30	26213.
1.07	22111.
1.05	21780.
1.04	21742.
0.85	18105.
0.81	17674.
0.81	17576.
0.60	13345.
0.59	13113.
0.59	12839.
0.38	9525.
0.36	9461.

5.55	110750.
5.56	110846.
5.57	110887.
5.31	105007.
5.31	105261.
5.32	105316.
5.04	99384.
5.04	99412.
5.05	99403.
4.77	93858.
4.77	93901.
4.77	93840.
4.48	87913.
4.47	88021.
4.49	88036.
4.17	81843.
4.17	81843.
4.16	81811.
3.87	76302.
3.87	76340.
3.87	76506.
3.59	70714.
3.59	70805.
3.58	70755.
3.30	65473.
3.30	65566.
3.31	65676.
3.04	60363.
3.04	60354.
3.04	60332.
2.78	55164.
2.78	55030.
2.79	54944.
2.53	50097.
2.52	49984.
2.53	50135.
2.29	45379.
2.28	45308.
2.28	45205.
2.03	40447.
2.04	40383.
2.04	40356.
1.79	35241.
1.78	35058.
1.77	34917.
1.51	30508.
1.50	30309.
1.49	30263.
1.28	26088.
1.28	25981.
1.28	25956.
1.04	21952.
1.03	21664.
1.02	21510.
0.81	17554.
0.79	17321.
0.79	17247.
0.62	13705.
0.59	13271.
0.59	13189.

R134a/2Al0 (99/1)
File: TBCAL81.dat

ΔT_s (K)	q'' (W/m^2)
5.94	110548.
5.93	110718.
5.93	110844.
5.60	104410.
5.60	104760.
5.62	104951.
5.30	99080.
5.32	99209.
5.32	99209.
5.01	93418.
5.03	93509.
5.02	93497.
4.72	87776.
4.72	87901.
4.73	87900.
4.43	82193.
4.42	82166.
4.42	82341.
4.14	76724.
4.14	76679.
4.13	76738.
3.84	71071.
3.84	71064.
3.83	71070.
3.54	65569.
3.54	65565.
3.54	65602.
3.25	60277.
3.25	60322.
3.25	60368.
2.96	55054.
2.97	55114.
2.96	55064.
2.70	50094.
2.69	49998.
2.68	49983.
2.41	44919.
2.40	44826.
2.40	44911.
2.13	39794.
2.11	39703.
2.11	39711.
1.85	34963.
1.83	34886.
1.84	34977.
1.60	30602.
1.59	30521.
1.58	30454.
1.35	26164.
1.35	26035.
1.35	25950.
1.13	21869.
1.10	21500.
1.10	21346.
0.88	17767.
0.84	17263.
0.84	17175.
0.63	13924.
0.60	13547.
0.60	13528.
0.44	9569.
0.43	9200.
5.80	110207.
5.79	110965.
5.80	111047.
5.50	105071.
5.51	105202.
5.51	105230.
5.23	99382.
5.23	99166.
5.23	99155.
4.93	93274.
4.92	93415.
4.92	93573.
4.64	87996.
4.65	88227.
4.66	88028.
4.34	82115.
4.34	82014.
4.34	82066.
4.05	76695.
4.05	76743.
4.03	76714.
3.77	71157.
3.77	71135.
3.77	71031.
3.48	65720.
3.48	65525.
3.48	65605.
3.19	60321.
3.17	60397.
3.18	60364.
2.89	55080.
2.89	55063.
2.90	54961.
2.62	50089.
2.62	50127.
2.61	50090.
2.34	45142.
2.32	44950.
2.31	44899.
2.06	39892.
2.05	39691.
2.06	39639.
1.78	34775.
1.78	34827.
1.78	34790.
1.55	30531.
1.55	30220.
1.55	30297.
1.33	26201.
1.32	25985.
1.32	25927.
1.08	21745.
1.06	21601.
1.05	21519.
0.84	17873.
0.81	17463.
0.82	17397.
0.62	13714.
0.60	13340.
0.60	13333.
0.41	9869.
0.39	9551.
5.66	111778.
5.67	111544.
5.67	111605.
5.38	105285.
5.39	105309.
5.40	105390.
5.11	99524.
5.12	99595.
5.12	99671.
4.83	93761.
4.84	93742.
4.84	93733.
4.58	87949.
4.58	87927.
4.57	87953.
4.28	82244.
4.29	82275.
4.29	82338.
4.00	76635.
4.00	76758.
4.00	76799.
3.73	71248.
3.71	71167.
3.72	71220.
3.42	65748.
3.42	65631.
3.41	65518.
3.12	60162.
3.12	60341.
3.12	60337.
2.86	55247.
2.85	55103.
2.85	55181.
2.60	50136.
2.59	50137.
2.58	50117.
2.33	44634.
2.31	44446.
2.31	44405.
2.05	40190.
2.04	40013.
2.04	39915.
1.78	34854.
1.79	35071.
1.79	35021.
1.55	30618.
1.54	30378.
1.55	30421.
1.30	26001.
1.31	26102.
1.31	26045.
1.07	21833.
1.06	21420.
1.05	21275.
0.84	17506.
0.82	17259.
0.82	17190.
0.61	13825.
0.58	13549.
0.59	13481.
0.43	9827.
0.40	9252.
5.61	111718.
5.63	111864.
5.62	111305.

5.35	105244.
5.35	105269.
5.36	105429.
5.15	99485.
5.17	98702.
5.16	99799.
4.88	93606.
4.89	93742.
4.88	94032.
4.59	88178.
4.60	88179.
4.61	88329.
4.30	82218.
4.30	82444.
4.31	82529.
4.02	76698.
4.01	76758.
4.01	76469.
3.71	71351.
3.73	71402.
3.73	71084.
3.42	65561.
3.42	65691.
3.42	65916.
3.13	60236.
3.14	60453.
3.15	60382.
2.85	55235.
2.86	54910.
2.86	55288.
2.59	50252.
2.58	49938.
2.58	49798.
2.30	44749.
2.29	44548.
2.29	44554.
2.01	39869.
2.01	39902.
2.02	40167.
1.78	35125.
1.78	35311.
5.65	111632.
5.66	111694.
5.67	111814.
5.40	104619.
5.38	105370.
5.38	105669.
5.10	99783.
5.09	99816.
5.10	99884.
4.83	94262.
4.84	94231.
4.83	94165.
4.56	88398.
4.55	88508.
4.57	88520.
4.27	82413.
4.27	82438.
4.28	82424.
3.98	76798.
3.98	76870.
3.98	76820.
3.70	71256.
3.69	71218.
3.68	71216.

3.41	65889.
3.41	65984.
3.41	66075.
3.14	60579.
3.14	60599.
3.13	60607.
2.86	55220.
2.86	55163.
2.87	54989.
2.60	50261.
2.59	50297.
2.60	50384.
2.35	44867.
2.34	44802.
2.33	44588.
2.04	40134.
2.04	40112.
2.05	40036.
1.80	35192.
1.80	35188.
1.80	34964.
1.56	30435.
1.56	30259.
1.55	30212.
1.32	26042.
1.33	26018.
1.32	25777.
1.11	21970.
1.07	21648.
1.07	21674.
0.87	18010.
0.84	17517.
0.85	17581.
0.63	13527.
0.60	13249.
0.61	13239.
0.41	9712.
0.40	9593.
5.86	112087.
5.88	112324.
5.90	112146.
5.62	105729.
5.61	105654.
5.62	105618.
5.33	99686.
5.34	99836.
5.34	99943.
5.07	94141.
5.07	94233.
5.08	94365.
4.80	88252.
4.80	88245.
4.82	88075.
4.53	82650.
4.52	82921.
4.52	82909.
4.24	77223.
4.23	77255.
4.23	77227.
3.93	71678.
3.92	71739.
3.93	71683.
3.63	66136.
3.63	66182.
3.62	66124.

3.33	60830.
3.33	60828.
3.33	60789.
3.03	55544.
3.03	55431.
3.01	55442.
2.73	50080.
2.73	50204.
2.73	50105.
2.43	45080.
2.42	45141.
2.43	45174.
2.15	39765.
2.15	39511.
2.14	39413.
1.85	35233.
1.86	35328.
1.86	35232.
1.61	30536.
1.61	30255.
1.61	30208.
1.36	25758.
1.36	25655.
1.36	25522.
1.10	21298.
1.08	21130.
1.08	21090.
0.84	17302.
0.83	17172.
5.72	111639.
5.75	111890.
5.76	111751.
5.46	105425.
5.46	105565.
5.48	105584.
5.20	99470.
5.21	99693.
5.22	99673.
4.93	93564.
4.94	93786.
4.94	93918.
4.67	88434.
4.67	88535.
4.66	88505.
4.39	82547.
4.37	82478.
4.38	82637.
4.09	76886.
4.09	76967.
4.10	76958.
3.80	71368.
3.80	71525.
3.80	71514.
3.53	66065.
3.52	66027.
3.53	66081.
3.24	60553.
3.23	60507.
3.23	60452.
2.95	55432.
2.94	55417.
2.95	55494.
2.68	50432.
2.67	50387.
2.67	50365.

2.40	44907.
2.39	44875.
2.40	44792.
2.11	40084.
2.09	39956.
2.10	39955.
1.84	35375.
1.83	35391.
1.84	35274.
1.60	30595.
1.60	30424.
1.59	30253.
1.32	26094.
1.33	26182.
1.34	26306.
1.11	22147.
1.11	21990.
1.10	21798.
0.87	17967.
0.86	17544.
0.85	17655.
0.64	13977.
0.61	13676.
0.61	13617.
0.44	9699.
0.43	9377.
5.65	111056.
5.65	111006.
5.68	111059.
5.41	104849.
5.43	105058.
5.43	105020.
5.15	99393.
5.17	99494.
5.17	99487.
4.89	93728.
4.89	93769.
4.90	93803.
4.61	87987.
4.62	87938.
4.63	87328.
4.33	82389.
4.33	82269.
4.34	82311.
4.04	76458.
4.04	76563.
4.05	76541.
3.75	71262.
3.76	71424.
3.76	71482.
3.48	65921.
3.48	65781.
3.49	65603.
3.19	60358.
3.18	60399.
3.18	60392.
2.91	55291.
2.90	55418.
2.91	55514.
2.65	50180.
2.66	50250.
2.64	50221.
2.38	45068.
2.37	44834.
2.38	44983.

2.09	40241.
2.08	40210.
2.08	40143.
1.83	35336.
1.83	35441.
1.83	35440.
1.59	30847.
1.58	30701.
1.58	30604.
1.35	26342.
1.33	26006.
1.33	25909.
1.09	21942.
1.06	21643.
1.06	21551.
0.85	17807.
0.83	17588.
0.82	17408.
0.62	13700.
0.60	13328.
0.59	13385.
0.41	9873.
0.39	9562.
5.61	111429.
5.64	111698.
5.66	111928.
5.39	105416.
5.41	105438.
5.43	105466.
5.14	99385.
5.14	99373.
5.15	99323.
4.88	93763.
4.88	93855.
4.88	93892.
4.61	87384.
4.59	88012.
4.61	88108.
4.31	82357.
4.33	81433.
4.32	82468.
4.04	76769.
4.03	76799.
4.02	76715.
3.74	71143.
3.73	71200.
3.74	71105.
3.44	65755.
3.43	65525.
3.45	65753.
3.15	60394.
3.14	60333.
3.15	60255.
2.85	55266.
2.86	55404.
2.87	55316.
2.62	49974.
2.61	49880.
2.62	49905.
2.33	44998.
2.33	44904.
2.33	44951.
2.07	39865.
2.05	39951.
2.05	39896.

1.80	35225.
1.79	35013.
1.79	35217.
1.54	30520.
1.55	30411.
1.53	30347.
1.31	26039.
1.29	25717.
1.29	25557.
1.06	21940.
1.04	21659.
1.04	21575.
0.84	17916.
0.82	17652.
0.82	17544.
0.62	13832.
0.59	13371.
0.58	13264.
0.39	9629.
0.38	9428.
5.77	111716.
5.77	111733.
5.78	111541.
5.51	104306.
5.50	105270.
5.49	105319.
5.23	98350.
5.22	99326.
5.22	99244.
4.93	93777.
4.93	93633.
4.93	93745.
4.65	88029.
4.66	88130.
4.65	88090.
4.36	82244.
4.36	82138.
4.37	82324.
4.07	76606.
4.06	76740.
4.07	76723.
3.78	71410.
3.78	71571.
3.79	71693.
3.50	66087.
3.50	66023.
3.50	66079.
3.22	60671.
3.20	60632.
3.21	60639.
2.92	55507.
2.91	55446.
2.92	55432.
2.63	50172.
2.64	50218.
2.63	50176.
2.35	45192.
2.35	45160.
2.33	45073.
2.07	39922.
2.05	39761.
2.05	39620.
1.79	35263.
1.77	35200.
1.77	35182.

1.55	30402.
1.54	30406.
1.54	30370.
1.30	26331.
1.27	26187.
1.29	26181.
1.06	21339.
1.06	21137.
5.79	110694.
5.79	110534.
5.81	110246.
5.53	104385.
5.58	99872.
5.52	104658.
5.25	98862.
5.26	98792.
5.25	98835.
4.96	93179.
4.97	93121.
4.98	93146.
4.69	87640.
4.69	87631.
4.69	87521.
4.41	81660.
4.39	81622.
4.39	81738.
4.11	76287.
4.11	76207.
4.11	76271.
3.84	70777.
3.83	70809.
3.85	70930.
3.56	65412.
3.54	65124.
3.54	65189.
3.18	57849.
3.09	57058.
3.20	58774.
2.96	54423.
2.96	54460.
2.97	54527.
2.69	49677.
2.67	49409.
2.67	49435.
2.42	44261.
2.39	44322.
2.38	44104.
2.14	39594.
2.11	39213.
2.10	39270.
1.86	34614.
1.84	34603.
1.85	34588.
1.61	30093.
1.60	29908.
1.58	29684.
1.38	25505.
1.38	25288.
1.37	25168.
1.04	20027.
1.11	21047.
5.68	111593.
5.67	111869.
5.70	110925.
5.40	104482.

5.39	104742.
5.42	105080.
5.13	98717.
5.13	98693.
5.13	99236.
4.84	93522.
4.85	93791.
4.86	93861.
4.61	88071.
4.61	87787.
4.61	88240.
4.20	79963.
4.28	81282.
4.34	80494.
3.87	73102.
3.97	75448.
4.03	76355.
3.78	71007.
3.77	71361.
3.78	71253.
3.50	65532.
3.49	65453.
3.49	65498.
3.21	59982.
3.21	59749.
3.20	59996.
2.91	54970.
2.91	55106.
2.92	54991.
2.65	49841.
2.76	49337.
2.73	49594.
2.42	44579.
2.41	44445.
2.41	44392.
2.14	39602.
2.12	39386.
2.11	39195.
1.87	34488.
1.85	34468.
1.92	33834.
1.61	29968.
1.61	30057.
1.62	30069.
1.40	25411.
5.68	110802.
5.67	111665.
5.70	111728.
5.41	104866.
5.41	104974.
5.40	104951.
5.12	99084.
5.13	99186.
5.12	99208.
4.85	92946.
4.85	93658.
4.74	91467.
4.56	87936.
4.58	88044.
4.58	88125.
4.29	82293.
4.29	82291.
4.29	82282.
4.02	76356.
4.02	76362.

4.02	76303.
3.74	71061.
3.73	71120.
3.74	71218.
3.46	65653.
3.45	65674.
3.45	65670.
3.16	60219.
3.16	60230.
3.16	60242.
2.88	55041.
2.88	54978.
2.87	54925.
2.61	49865.
2.60	49650.
2.59	49645.
2.33	44744.
2.32	44583.
2.32	44615.
2.07	39843.
2.05	39688.
2.05	39743.
1.82	34729.
1.80	34592.
1.81	34582.
1.57	30014.
1.55	29771.
1.56	29748.
1.32	25747.
1.31	25636.
1.30	25609.
1.10	21902.
1.07	21404.
1.06	21362.
0.87	17704.
0.86	17433.
0.85	17226.
0.64	13382.
0.62	13228.
0.62	13084.

R134a/5Al0 (99/1)
File: TBCAL17.dat

ΔT_s (K)	q'' (W/m^2)
6.50	106979.
6.49	106675.
6.49	106483.
6.24	100731.
6.24	100855.
6.26	100942.
6.00	95112.
5.98	95170.
6.00	95176.
5.72	89359.
5.71	89315.
5.72	89363.
5.43	83463.
5.42	83453.
5.43	83449.

5.10	77446.
5.09	77369.
5.10	77415.
4.82	72015.
4.82	72069.
4.82	72159.
4.53	66554.
4.53	66515.
4.53	66466.
4.22	61317.
4.22	61341.
4.22	61368.
3.88	55926.
3.88	55951.
3.88	55921.
3.58	51123.
3.57	51217.
3.59	51207.
3.27	46506.
3.27	46522.
3.27	46486.
2.92	41726.
2.93	41736.
2.93	41664.
2.60	37205.
2.60	37212.
2.58	37133.
2.29	32849.
2.27	32701.
2.27	32665.
1.98	28439.
1.94	28236.
1.95	28187.
1.64	23905.
1.63	23919.
1.63	23921.
1.34	20106.
1.33	19974.
1.32	19985.
1.10	16755.
1.05	16338.
1.04	16252.
0.78	12565.
0.76	12430.
6.86	105619.
6.87	105871.
6.88	106080.
6.53	99465.
6.53	99491.
6.52	99435.
6.18	93484.
6.18	93631.
6.18	93586.
5.83	88053.
5.83	88041.
5.84	88078.
5.50	82593.
5.50	82627.
5.50	82625.
5.17	77245.
5.17	77320.
5.17	77429.
4.84	72150.
4.85	72209.
4.86	72277.

4.53	67046.
4.53	67179.
4.55	67276.
4.21	61885.
4.21	61786.
4.21	61755.
3.87	56466.
3.88	56538.
3.87	56521.
3.54	51605.
3.54	51628.
3.54	51594.
3.21	46870.
3.22	46929.
3.22	47014.
2.89	42166.
2.88	42048.
2.88	41953.
2.56	37278.
2.54	37192.
2.55	37287.
2.26	33104.
2.25	33049.
2.25	33025.
1.96	28871.
1.95	28776.
1.95	28707.
1.67	24734.
1.65	24561.
1.66	24513.
1.38	20650.
1.35	20364.
1.35	20232.
1.09	16896.
1.06	16531.
6.69	106276.
6.70	106420.
6.70	106092.
6.35	99607.
6.35	99535.
6.36	99503.
6.03	94023.
6.03	94165.
6.03	94238.
5.71	88727.
5.71	88815.
5.72	88901.
5.38	83206.
5.38	83212.
5.38	83227.
5.04	77463.
5.04	77428.
5.04	77450.
4.72	71998.
4.72	72113.
4.73	72150.
4.39	66889.
4.39	66930.
4.40	66951.
4.08	61730.
4.06	61630.
4.07	61647.
3.73	56459.
3.74	56525.
3.73	56437.

3.42	51587.
3.41	51513.
3.41	51589.
3.10	46739.
3.10	46765.
3.10	46749.
2.77	41858.
2.77	41775.
2.76	41687.
2.46	37351.
2.44	37342.
2.45	37316.
2.18	32943.
2.17	32898.
2.16	32860.
1.90	28756.
1.88	28630.
1.87	28581.
1.61	24582.
1.59	24424.
1.59	24461.
1.35	20806.
1.31	20438.
1.31	20340.
1.07	16816.
1.05	16552.
6.59	106389.
6.60	106610.
6.61	106698.
6.28	100351.
6.27	100409.
6.28	100471.
5.96	94454.
5.95	94469.
5.96	94496.
5.63	88763.
5.64	88899.
5.63	88951.
5.32	83335.
5.32	83415.
5.31	83360.
4.99	77646.
4.99	77684.
4.99	77697.
4.68	72295.
4.69	72421.
4.69	72414.
4.38	66836.
4.37	66788.
4.36	66726.
4.04	61451.
4.05	61583.
4.04	61638.
3.74	56633.
3.74	56711.
3.74	56797.
3.44	51634.
3.43	51546.
3.41	51403.
3.09	46749.
3.10	46952.
3.11	47170.
2.80	41995.
2.77	41817.
2.78	41747.

2.48	37332.
2.45	37237.
2.47	37184.
2.18	33023.
2.18	32967.
2.18	32975.
1.92	28727.
1.90	28629.
1.90	28570.
1.62	24562.
1.61	24392.
1.61	24356.
1.35	20751.
1.33	20430.
1.32	20409.
1.08	16852.
1.06	16459.
6.52	106422.
6.52	106531.
6.51	106396.
6.20	100198.
6.19	100134.
6.19	100115.
5.86	94140.
5.86	94301.
5.87	94329.

5.55	88581.
5.55	88619.
5.55	88604.
5.24	82998.
5.23	82943.
5.23	82966.
4.91	77375.
4.91	77437.
4.91	77506.
4.60	72149.
4.61	72200.
4.61	72206.
4.30	66929.
4.30	67022.
4.31	67032.
3.98	61563.
3.98	61615.
3.98	61612.
3.66	56269.
3.66	56242.
3.65	56177.
3.34	51446.
3.34	51546.
3.36	51620.
3.05	46791.
3.04	46743.

3.05	46771.
2.73	41776.
2.73	41821.
2.73	41760.
2.44	37456.
2.43	37463.
2.43	37481.
2.17	33235.
2.16	33167.
2.16	33102.
1.89	29002.
1.87	28829.
1.87	28752.
1.59	24646.
1.58	24652.
1.58	24613.
1.31	20557.
1.30	20491.
1.30	20467.
1.05	16913.
1.03	16693.
1.03	16668.

Table 3 Number of test days and data points

Fluid (% mass fraction)	Number of days	Number of data points
Pure R134a 1.6 K ≤ ΔT_s ≤ 5.0 K	3	118
R134a/RL68H (99.5/0.5) 1. 7 K ≤ ΔT_s ≤ 5.6 K	5	212
R134a/RL68H (99/1) 0.6 K ≤ ΔT_s ≤ 6.0 K	8	359
R134a/1AlO (99.5/0.5) 0.4 K ≤ ΔT_s ≤ 5.2 K	7	402
R134a/1AlO (99/1) 0.4 K ≤ ΔT_s ≤ 5.8 K	7	420
R134a/2AlO (99/1) 0.4 K ≤ ΔT_s ≤ 5.8 K	13	749
R134a/5AlO (99/1) 0.8 K ≤ ΔT_s ≤ 6.7 K	5	284

Table 4 Estimated parameters for cubic boiling curve fits for Turbo-BII-HP copper surface

$\Delta T_s = A_0 + A_1 q" + A_2 q"^2 + A_3 q"^3$

ΔT_s in kelvin and $q"$ in W/m^2

Fluid	A_o	A_1	A_2	A_3
Pure R134a 1.6 K ≤ ΔT_s ≤ 5.0 K	0.107591	4.31453×10^{-5}	1.55837×10^{-10}	-1.27477×10^{-15}
R134a/RL68H (99.5/0.5) 1. 7 K ≤ ΔT_s ≤ 5.6 K	-0.213154	6.17060×10^{-5}	-1.31398×10^{-10}	3.94500×10^{-16}
R134a/RL68H (99/1) 0.6 K ≤ ΔT_s ≤ 6.0 K	-0.248401	7.09353×10^{-5}	-1.78672×10^{-10}	4.35663×10^{-16}
R134a/1AlO (99.5/0.5) 0.4 K ≤ ΔT_s ≤ 5.2 K	-0.190960	5.09350×10^{-5}	-3.05821×10^{-11}	2.50653×10^{-17}
R134a/1AlO (99/1) 0.4 K ≤ ΔT_s ≤ 5.8 K	-0.129380	5.59308×10^{-5}	-3.59544×10^{-11}	5.52927×10^{-17}
R134a/2AlO (99/1) 0.4 K ≤ ΔT_s ≤ 5.8 K	-0.117681	5.47738×10^{-5}	3.14180×10^{-11}	-4.54983×10^{-16}
R134a/5AlO (99/1) 0.8 K ≤ ΔT_s ≤ 6.7 K	-0.182003	7.63341×10^{-5}	-1.07500×10^{-10}	-7.00023×10^{-17}

Table 5 Residual standard deviation of ΔT_s

Fluid	(K)
Pure R134a 1.6 K ≤ ΔT_s ≤ 5.0 K	0.09
R134a/RL68H (99.5/0.5) 1. 7 K ≤ ΔT_s ≤ 5.6 K	0.03
R134a/RL68H (99/1) 0.6 K ≤ ΔT_s ≤ 6.0 K	0.03
R134a/1AlO (99.5/0.5) 0.4 K ≤ ΔT_s ≤ 5.2 K	0.09
R134a/1AlO (99/1) 0.4 K ≤ ΔT_s ≤ 5.8 K	0.07
R134a/2AlO (99/1) 0.4 K ≤ ΔT_s ≤ 5.8 K	0.06
R134a/5AlO (99/1) 0.8 K ≤ ΔT_s ≤ 6.7 K	0.09

Table 6 Average magnitude of 95 % multi-use confidence interval for mean ΔT_s

Fluid	U (K)
Pure R134a 1.6 K ≤ ΔT_s ≤ 5.0 K	0.06
R134a/RL68H (99.5/0.5) 1. 7 K ≤ ΔT_s ≤ 5.6 K	0.01
R134a/RL68H (99/1) 0.6 K ≤ ΔT_s ≤ 6.0 K	0.01
R134a/1AlO (99.5/0.5) 0.4 K ≤ ΔT_s ≤ 5.2 K	0.03
R134a/1AlO (99/1) 0.4 K ≤ ΔT_s ≤ 5.8 K	0.02
R134a/2AlO (99/1) 0.4 K ≤ ΔT_s ≤ 5.8 K	0.01
R134a/5AlO (99/1) 0.8 K ≤ ΔT_s ≤ 6.7 K	0.03

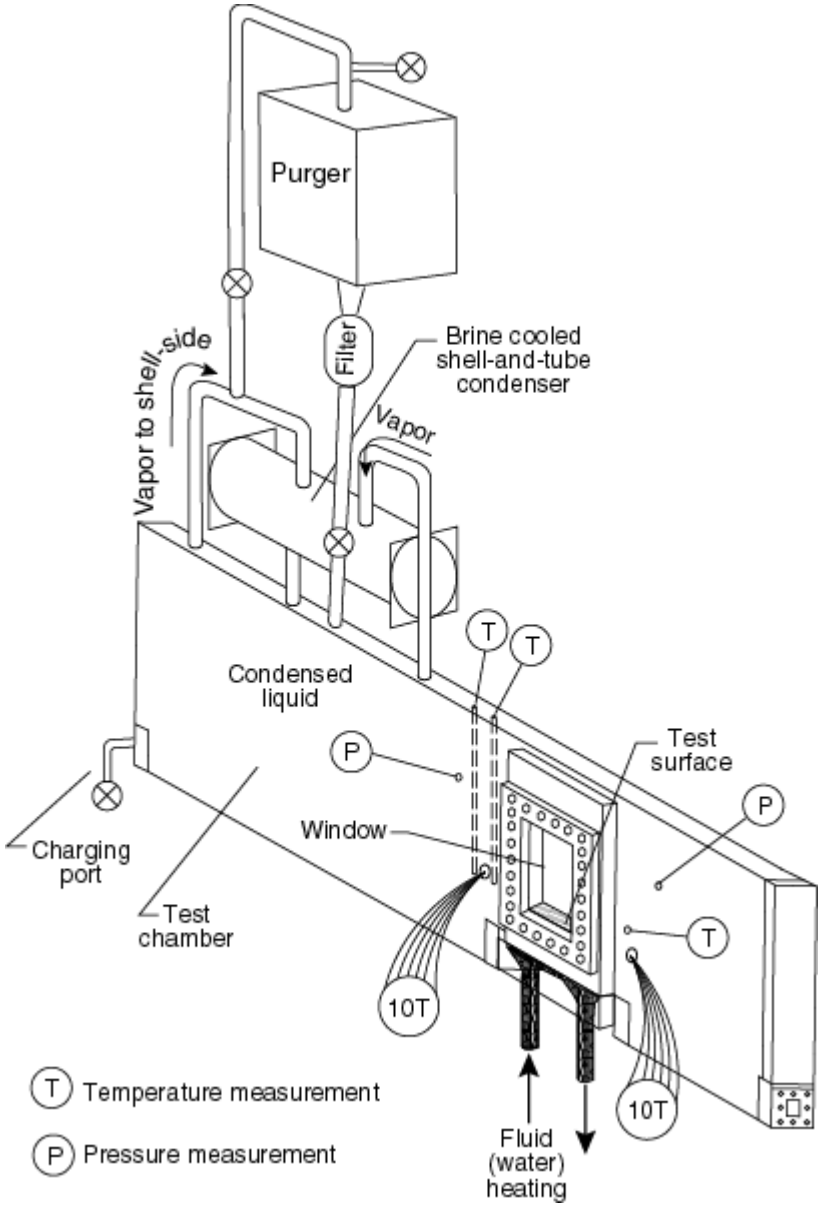

Fig. 1 Schematic of test apparatus

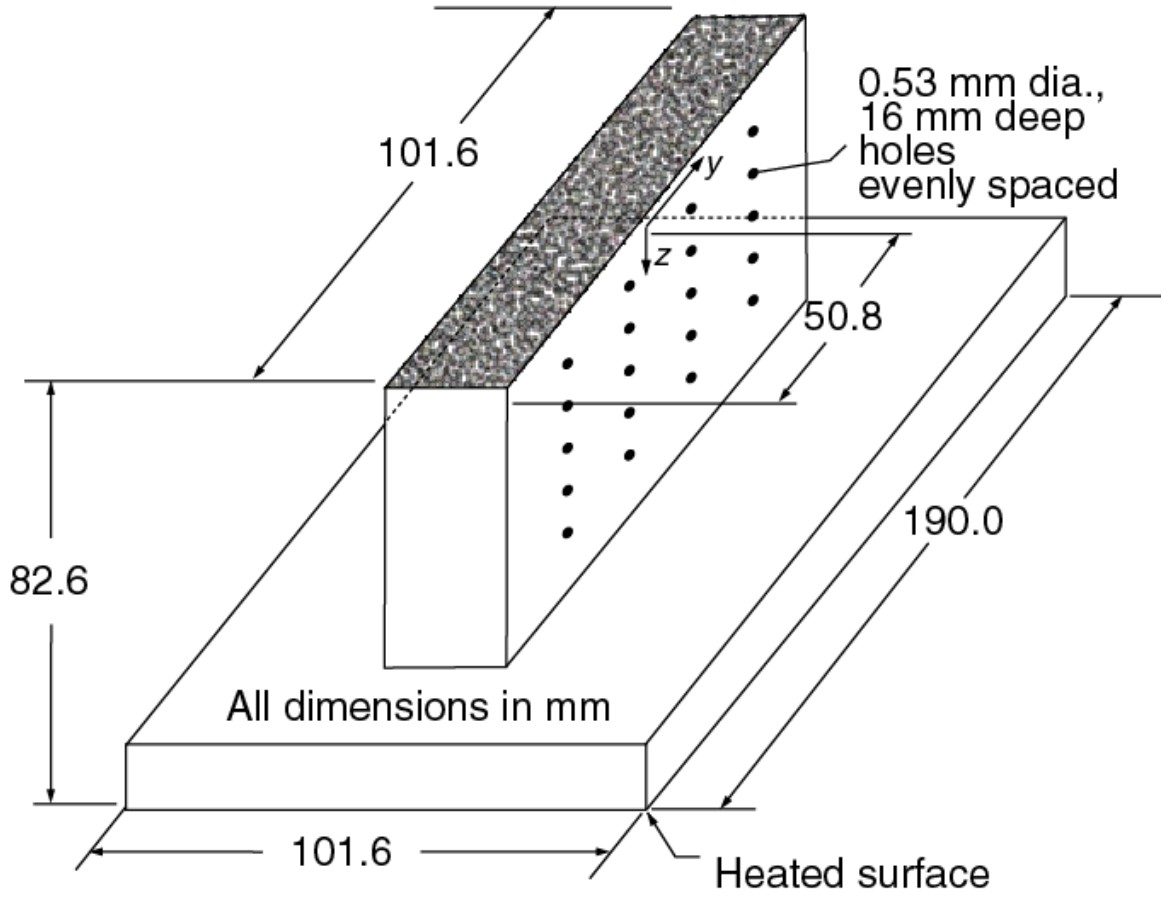

Fig. 2 OFHC copper flat test plate with Turbo-BII-HP surface and thermocouple coordinate system

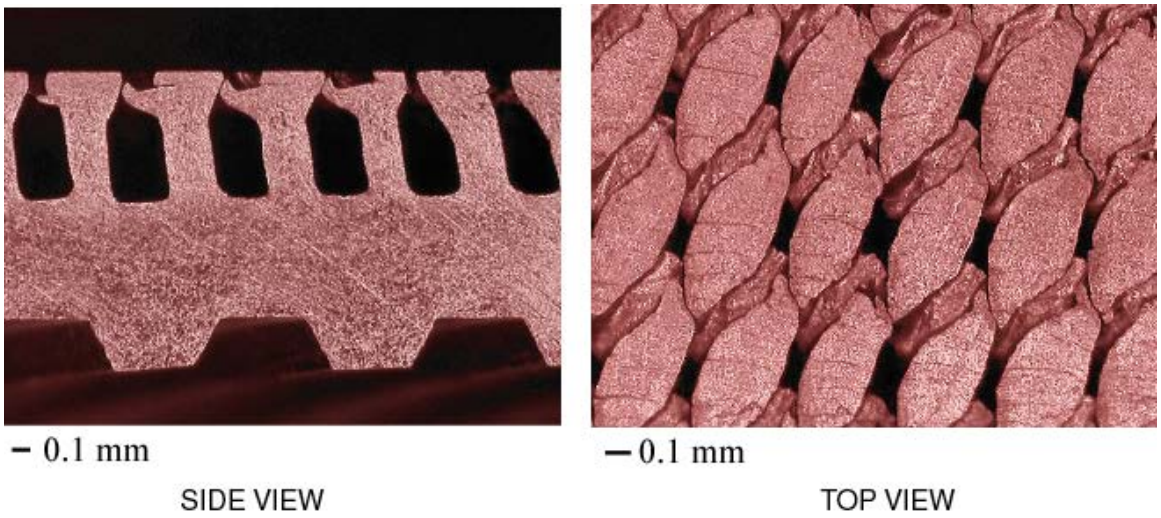

Fig. 3 Photograph of Turbo-BII-HP surface

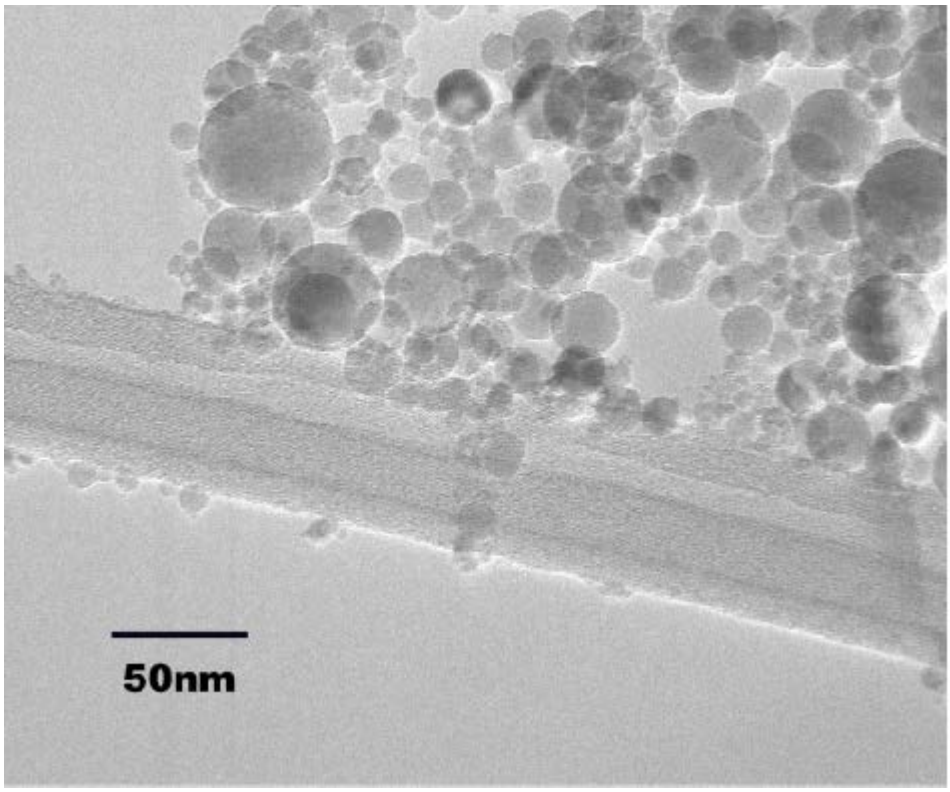

Fig. 4 TEM of Al_2O_3 nanolubricant (Sarkas, 2009)

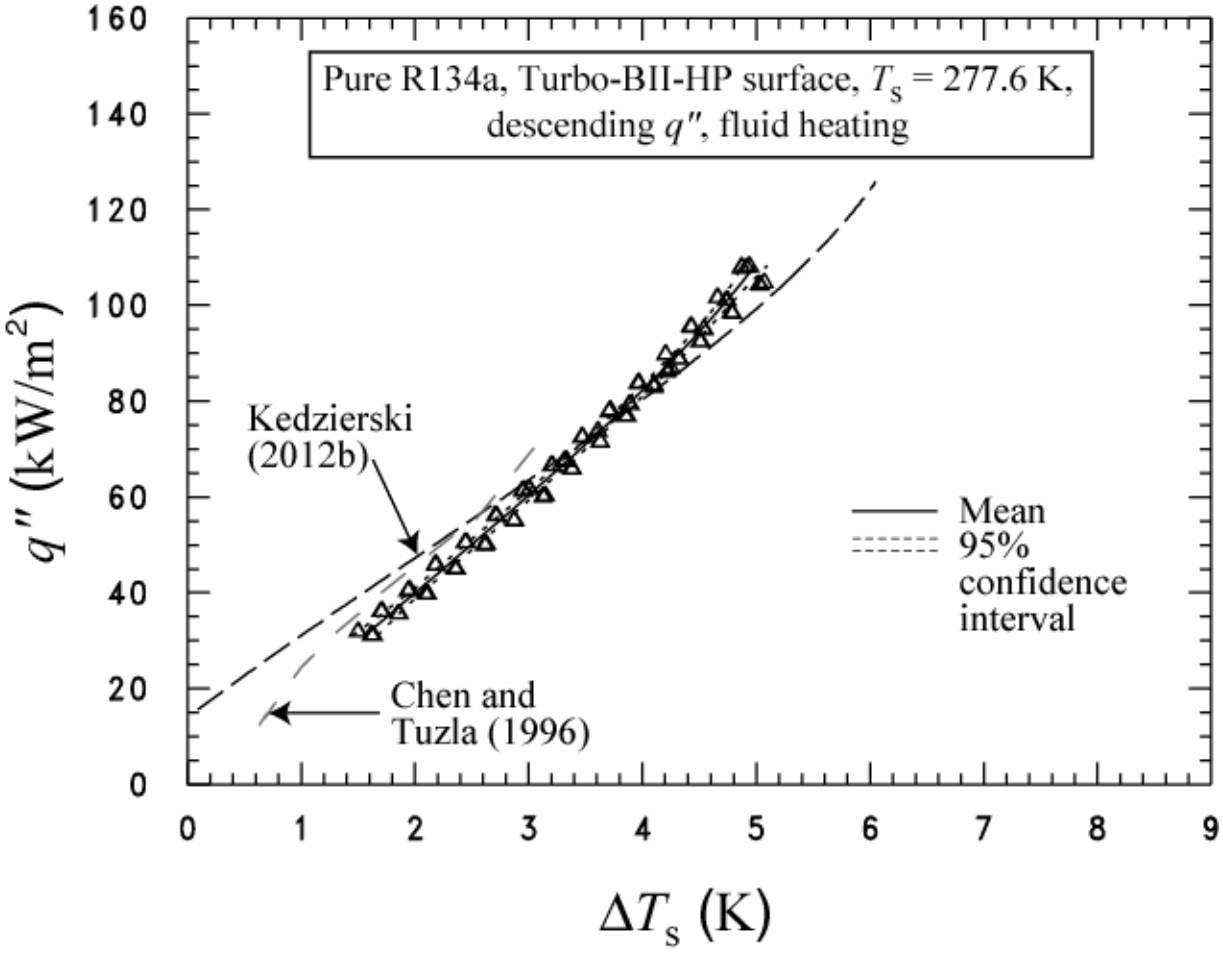

Fig. 5 Pure R134a boiling curve for Turbo-BII-HP

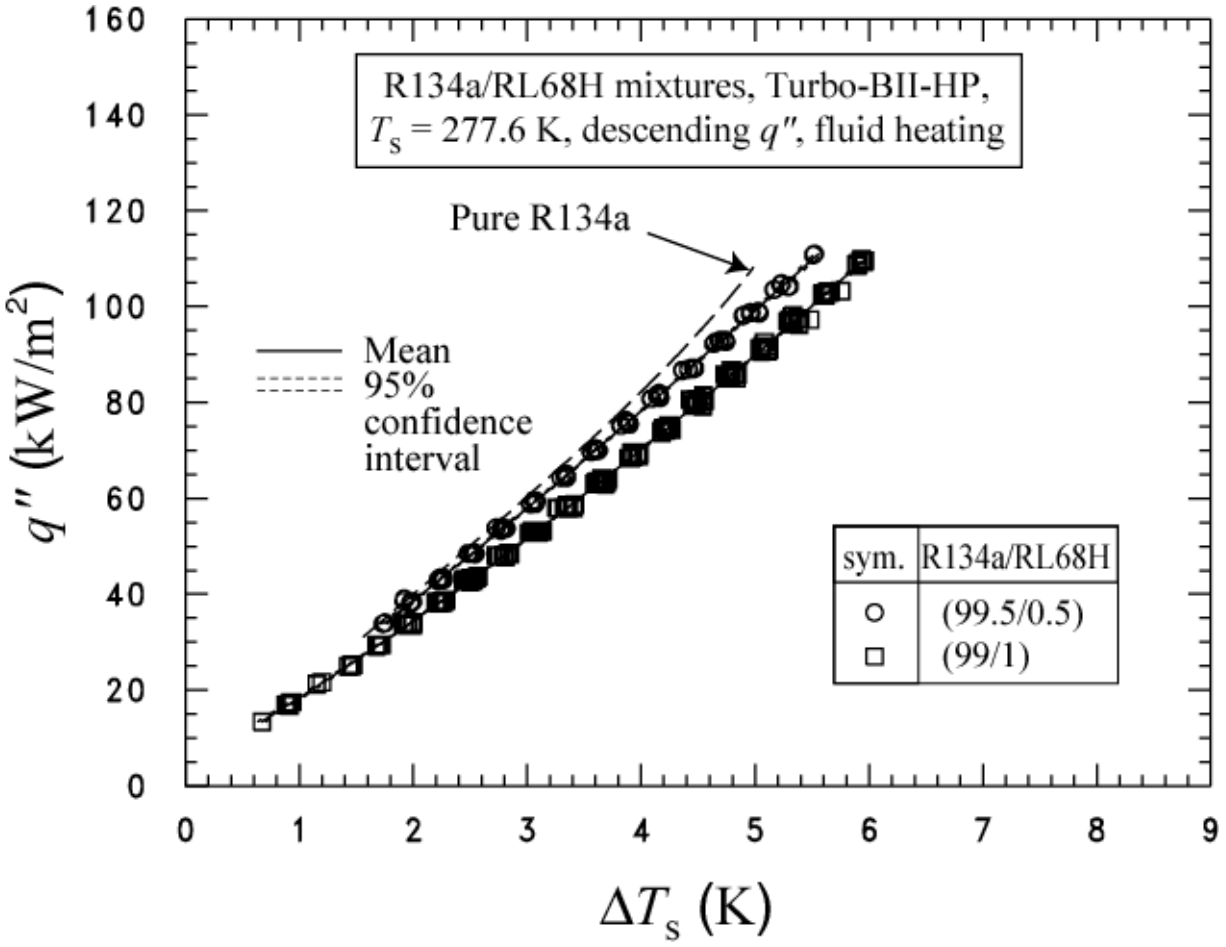

Fig. 6 R134a/RL68H mixtures boiling curves for Turbo-BII-HP

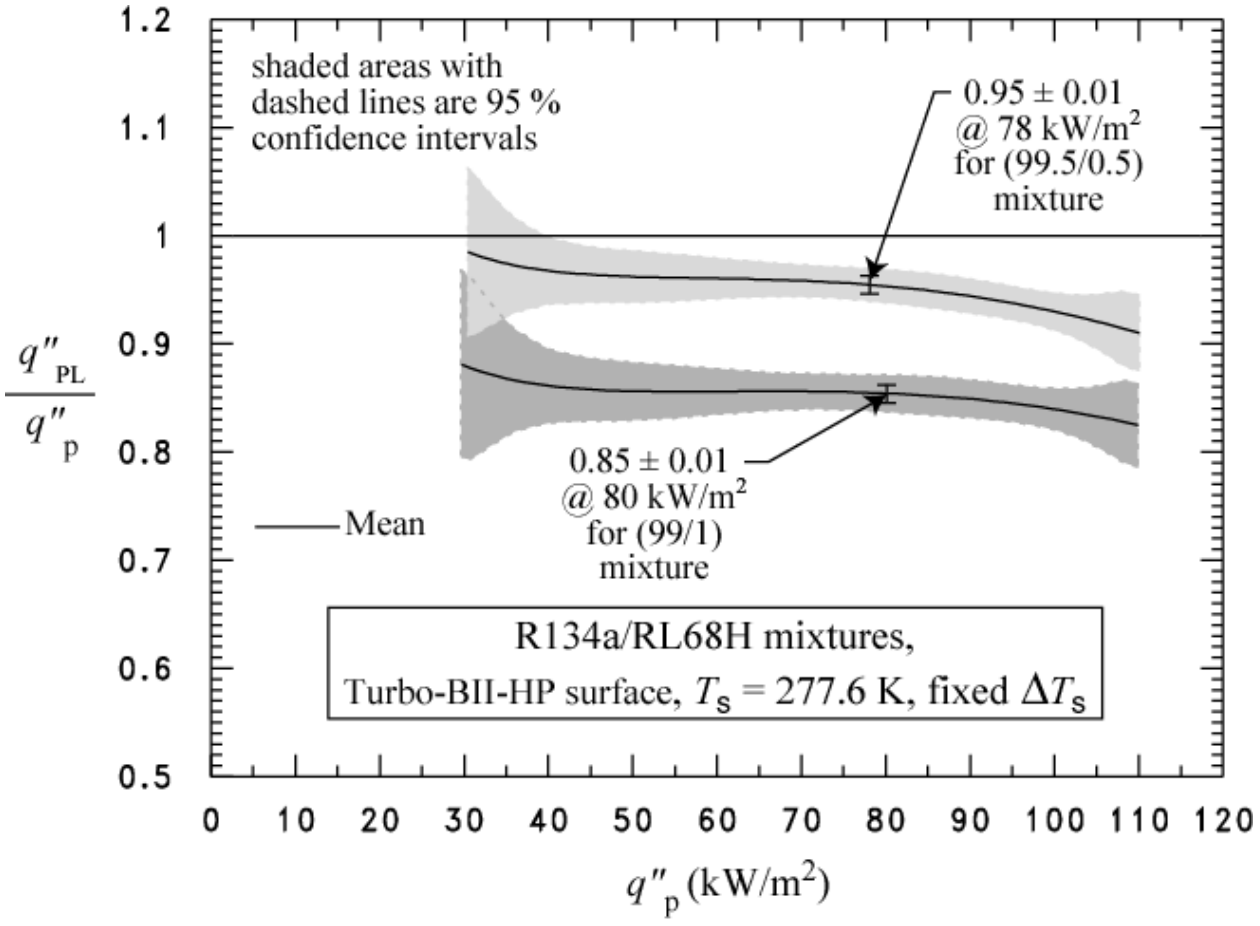

Fig. 7 Boiling heat flux of R134a/RL68H mixture relative to that of pure R134a for Turbo-BII-HP

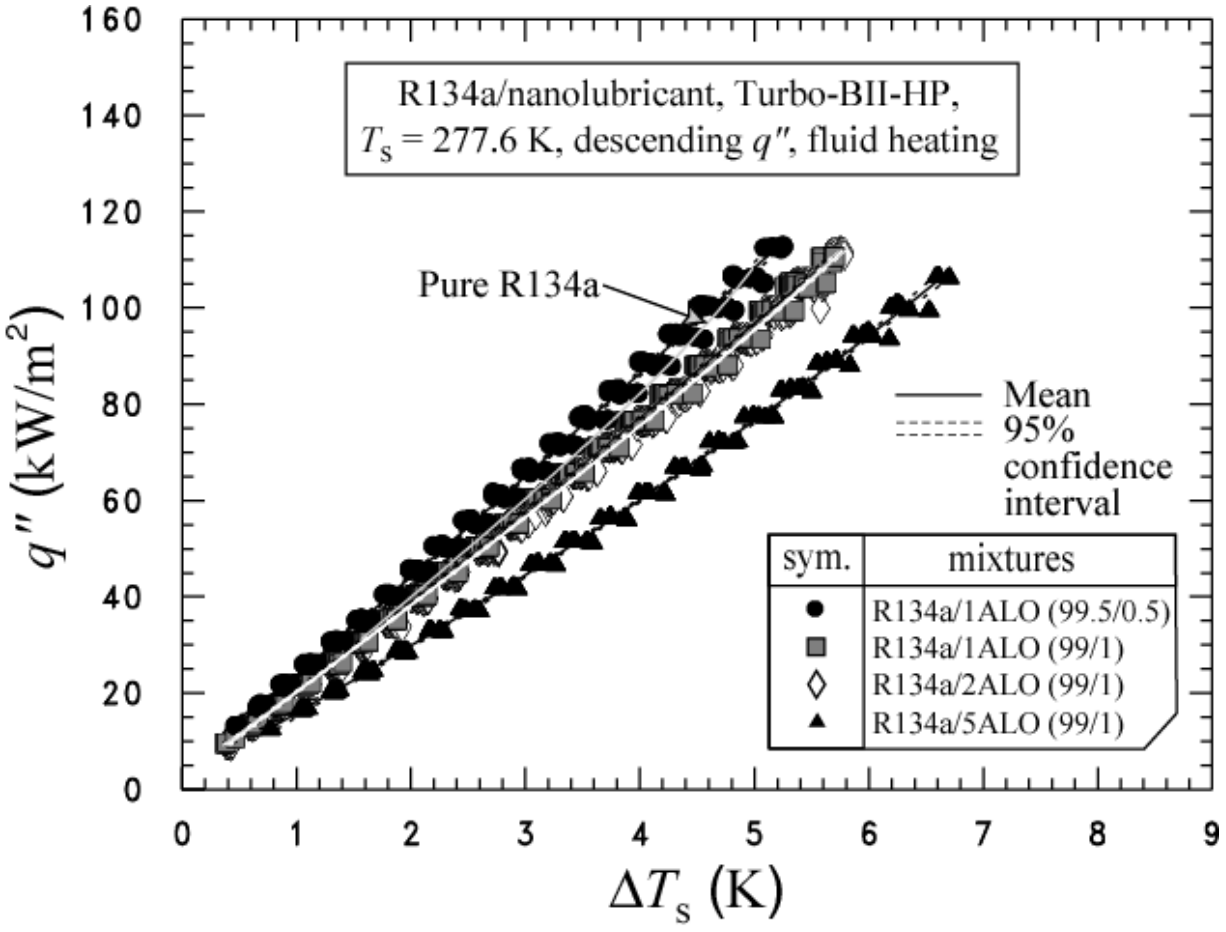

Fig. 8 R134a/RL68AlO mixtures boiling curves for Turbo-BII-HP

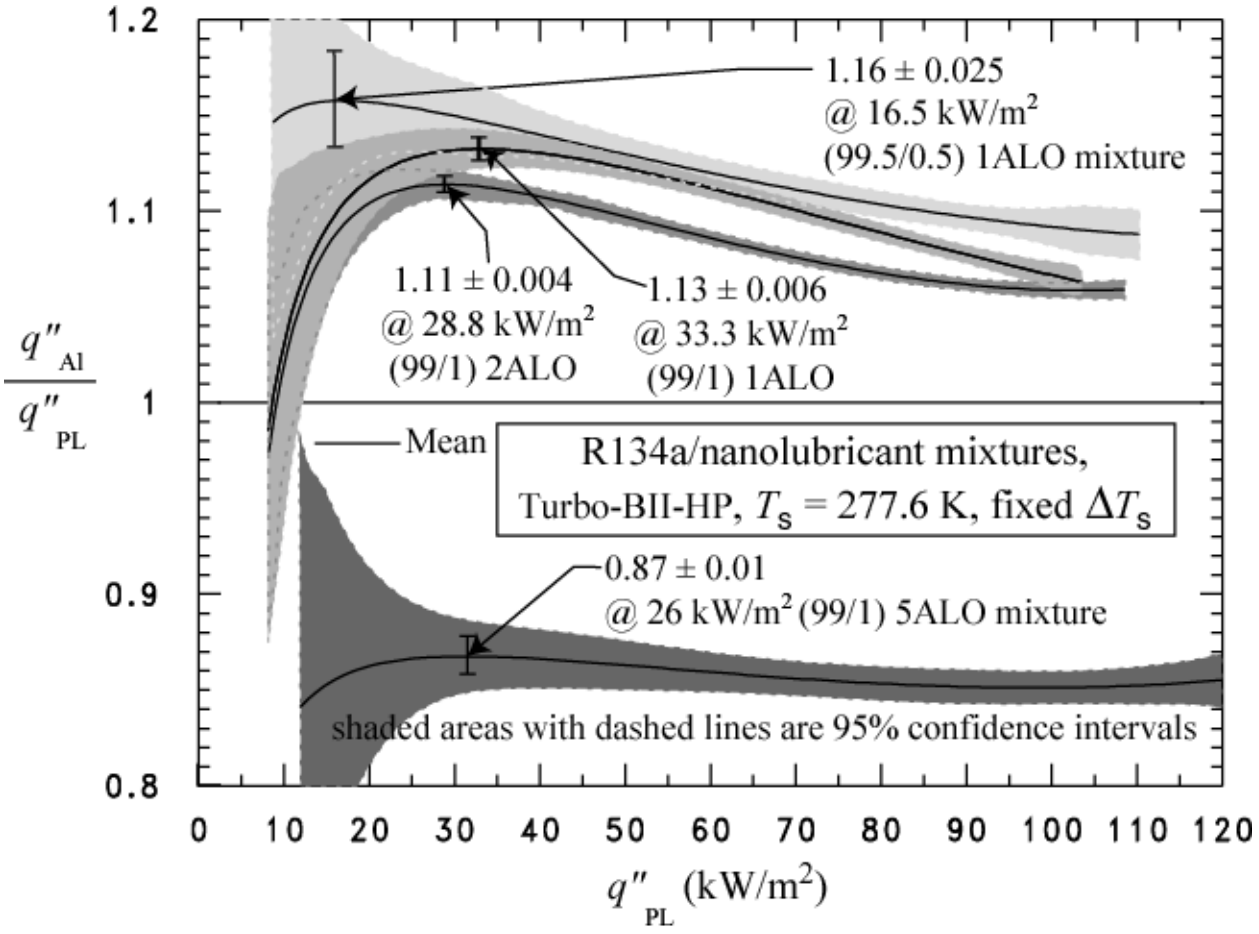

Fig. 9 Boiling heat flux of R134a/nanolubricant mixtures relative to that of R134a/RL68H without nanoparticles for Turbo-BII-HP

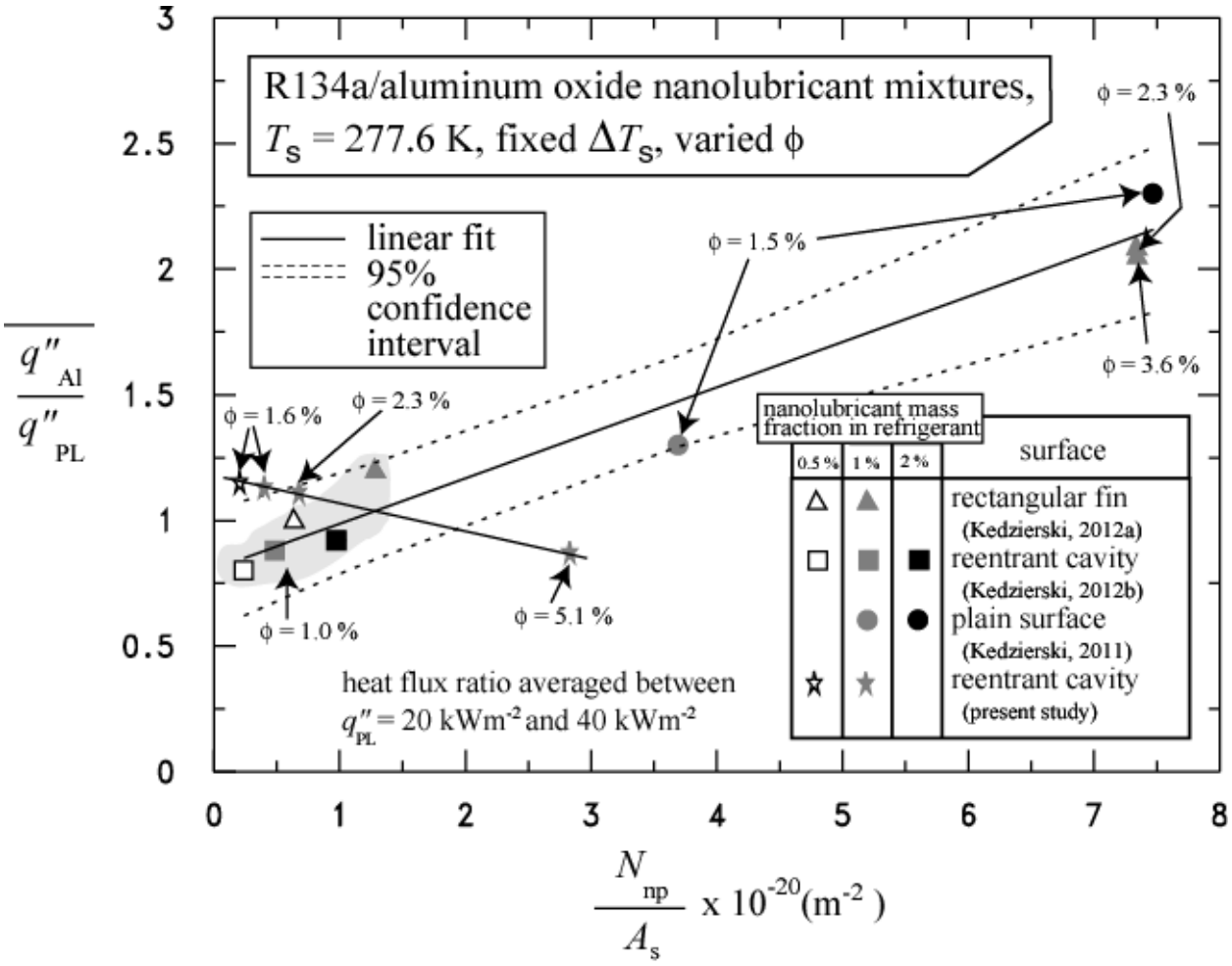

Fig. 10 Absolute number of nanoparticles determines average heat transfer enhancement for three different surfaces

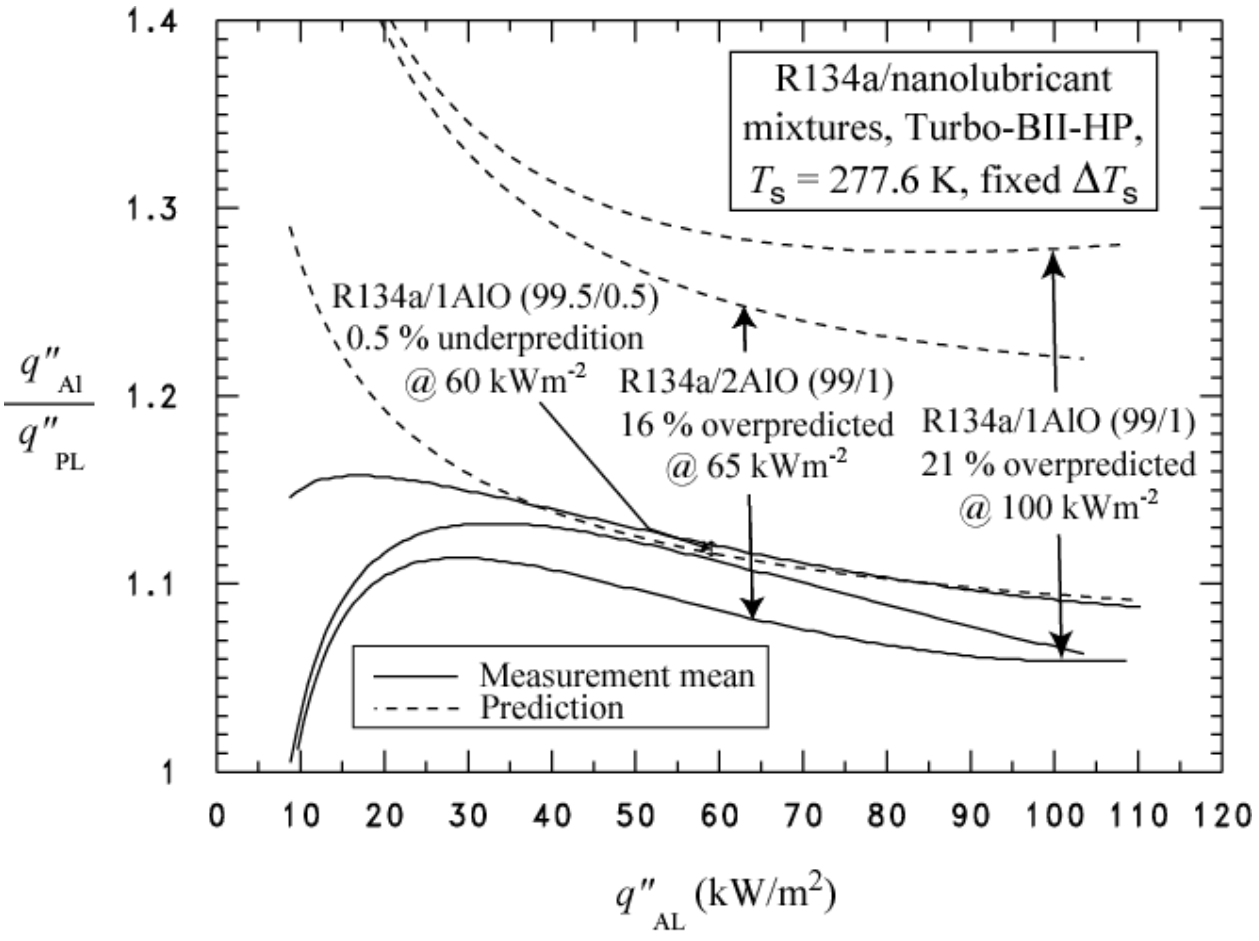

Fig. 11 Comparison of predicted to measured heat flux ratio for four different refrigerant/nanolubricant mixtures boiling on a Turbo-BII-HP

APPENDIX A: UNCERTAINTIES

Figure A.1 shows the relative (percent) uncertainty of the heat flux ($U_{q"}$) as a function of the heat flux. Figure A.2 shows the uncertainty of the wall temperature as a function of the heat flux. The uncertainties shown in Figs. A.1 and A.2 are "within-run uncertainties." These do not include the uncertainties due to "between-run effects" or differences observed between tests taken on different days. The "within-run uncertainties" include only the random effects and uncertainties associated with one particular test. All other uncertainties reported in this study are "between-run uncertainties" which include all random effects such as surface past history or seeding.

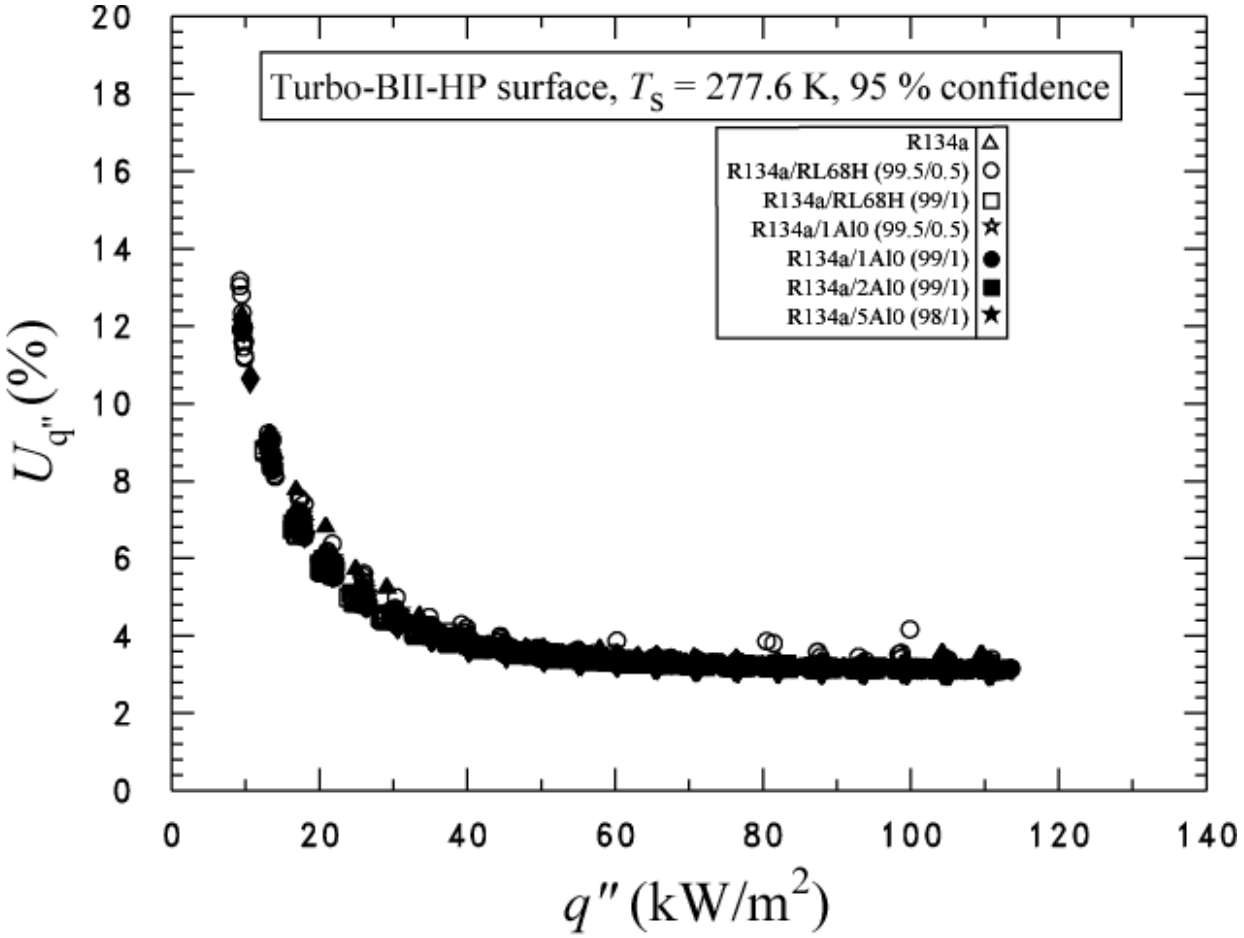

Fig. A.1 Expanded relative uncertainty in the heat flux of the surface at the 95 % confidence level

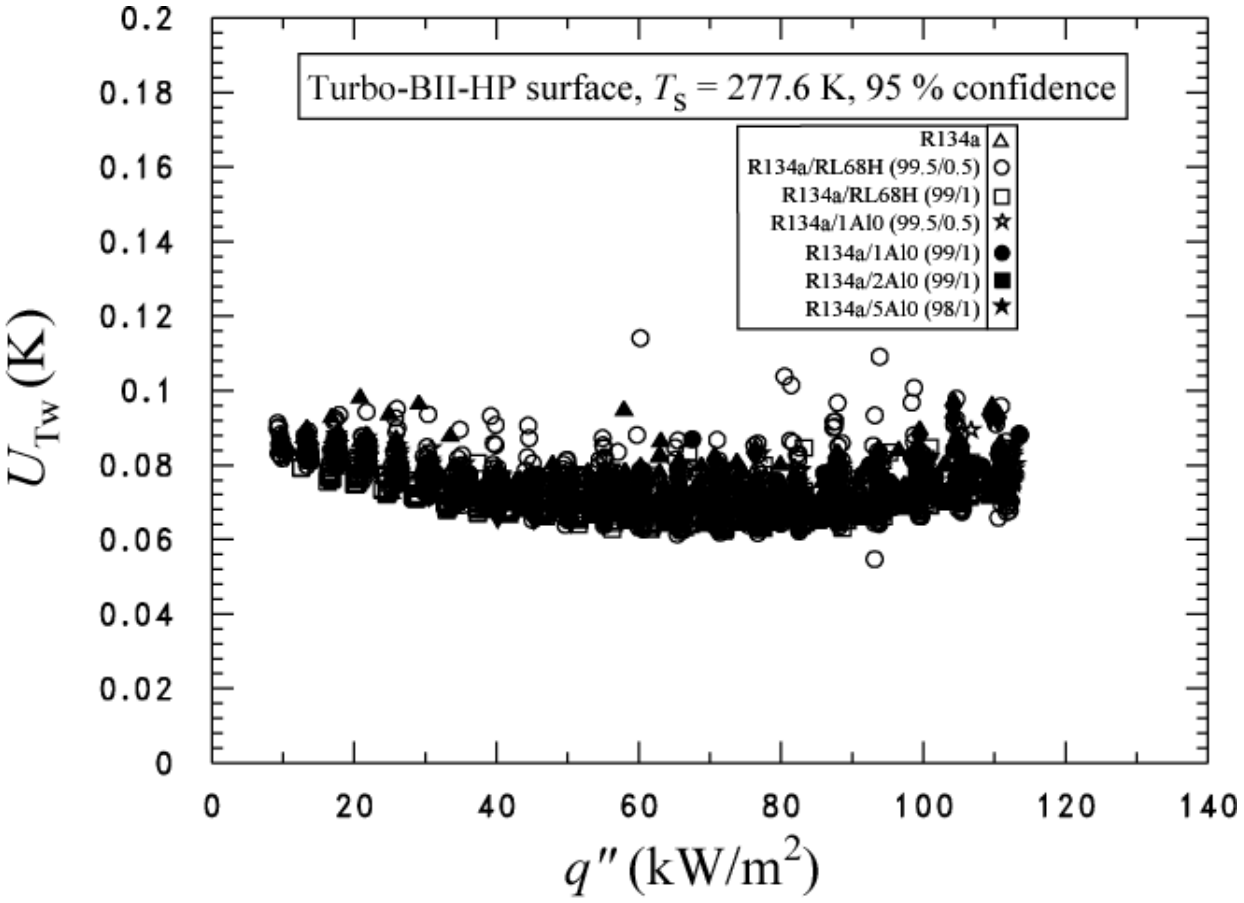

Fig. A.2 Expanded uncertainty in the temperature of the surface at the 95 % confidence level